Eur. Phys. J. C (2022) 82:461
https://doi.org/10.1140/epjc/s10052-022-10399-6

THE EUROPEAN PHYSICAL JOURNAL C

Check for updates

Regular Article - Theoretical Physics

Neutrino tomography of the Earth with ORCA detector

F. Capozzi[1,2], **S. T. Petcov**[3,4,5,a]

[1] Center for Neutrino Physics, Department of Physics, Virginia Tech, Blacksburg, VA 24061, USA
[2] Instituto de Fisica Corpuscular, Universidad de Valencia and CSIC, Edificio Institutos de Investigacion, Calle Catedratico Jose Beltran 2, 46980 Paterna, Spain
[3] SISSA/INFN, Via Bonomea 265, 34136 Trieste, Italy
[4] Kavli IPMU (WPI), UTIAS, The University of Tokyo, Kashiwa, Chiba 277-8583, Japan
[5] Institute of Nuclear Research and Nuclear Energy, Bulgarian Academy of Sciences, 1784 Sofia, Bulgaria

Received: 22 December 2021 / Accepted: 5 May 2022 / Published online: 20 May 2022
© The Author(s) 2022

Abstract Using PREM as a reference model for the Earth density distribution we investigate the sensitivity of ORCA detector to deviations of the Earth (i) outer core (OC) density, (ii) inner core (IC) density, (iii) total core density, and (iv) mantle density, from their respective PREM densities. The analysis is performed by studying the effects of the Earth matter on the oscillations of atmospheric ν_μ, ν_e, $\bar{\nu}_\mu$ and $\bar{\nu}_e$. We present results which illustrate the dependence of the ORCA sensitivity to the OC, IC, core and mantle densities on the type of systematic uncertainties used in the analysis, on the value of the atmospheric neutrino mixing angle θ_{23}, on whether the Earth mass constraint is implemented or not, and on the way it is implemented, and on the type – with normal ordering (NO) or inverted ordering (IO) – of the light neutrino mass spectrum. We show, in particular, that in the "most favorable" NO case of implemented Earth mass constraint, "minimal" systematic errors and $\sin^2\theta_{23} = 0.58$, ORCA can determine, e.g., the OC (mantle) density at 3σ C.L. after 10 years of operation with an uncertainty of $(-\ 18\%)/+\ 15\%$ (of $(-\ 6\%)/+\ 8\%$). In the "most disfavorable" NO case of "conservative" systematic errors and $\sin^2\theta_{23} = 0.42$, the uncertainty on OC (mantle) density reads $(-\ 43\%)/+\ 39\%$ ($(-\ 17\%/+\ 20\%)$, while for for $\sin^2\theta_{23} = 0.50$ and 0.58 it is noticeably smaller: $(-\ 37)\%/+\ 30\%$ and $(-\ 30\%)/+\ 24\%$ ($(-\ 13\%)/+\ 16\%$ and $(-\ 11\%/+\ 14\%)$). We find also that the sensitivity of ORCA to the OC, core and mantle densities is significantly worse for IO neutrino mass spectrum.

1 Introduction

A precise knowledge of the Earth's density distribution and of the average densities of the Earth's three different major structures – the mantle, outer core and inner core – is essential for understanding the physical conditions and fundamental aspects of the structure and properties of the Earth's interior (including the dynamics of mantle and core, the bulk composition of the Earth's three structures, the generation, properties and evolution of the Earth's magnetic field and the gravity field of the Earth) [1–4]. The thermal evolution of the Earth's core, in particular, depends critically on the density change across the inner core – outer core boundary (see, e.g., [5]).

At present our knowledge about the interior composition of the Earth and its density structure is based primarily on seismological and geophysical data (see, e.g., [3,6,7]). These data were used to construct the Preliminary Reference Earth Model (PREM) [8] of the density distribution of the Earth. In the PREM model, the Earth density distribution $\rho_{\rm E}$ is assumed to be spherically symmetric, $\rho_{\rm E} = \rho_{\rm E}(r)$, r being the distance from the Earth center, and there are two major density structures – the core and the mantle, and a certain number of substructures (shells or layers). The mantle has seven shells in the model, while the core is divided into an Inner Core (IC) and Outer Core (OC). The mean Earth radius is $R_\oplus = 6371$ km; the Earth core has a radius of $R_c = 3480$ km, with the IC and OC extending respectively from $r = 0$ to $r = 1221.5$ km, and from $r = 1221.5$ km to $r = 3480$ km. The mean densities of the mantle and the core are respectively $\bar{\rho}_{man} = 4.45$ g/cm^3 and $\bar{\rho}_c = 10.99$ g/cm^3.

The determination of the radial density distributions in the mantle and core, $\rho_{man}(r)$ and $\rho_c(r)$, from seismological and geophysical data is not direct and suffers from uncertainties [1,6,7]. An approximate and perhaps rather conservative estimate of this uncertainty for $\rho_{man}(r)$ is $\sim 5\%$; for the core density $\rho_c(r)$ it is larger and can be significantly larger [1,6,7] It was concluded in [7], in particular, that the density increase

[a] e-mail: petcov@sissa.it (corresponding author)

across the inner core – outer core boundary is known with an uncertainty of about 20%.

A unique alternative method of determination of the density profile of the Earth is the neutrino tomography of the Earth [9–24]. The propagation of the active flavour neutrinos and antineutrinos ν_α and $\bar{\nu}_\alpha$, $\alpha = e, \mu, \tau$, in the Earth is affected by the Earth matter. The original idea of neutrino Earth tomography is based on the observation that the cross section of the neutrino-nucleon interaction rises with energy. For neutrinos with energies $E_\nu \gtrsim$ a few TeV, the inelastic scattering off protons and neutrons leads to absorption of neutrinos and thus to attenuation of the initial neutrino flux. The magnitude of the attenuation depends on the Earth matter density profile along the neutrino path. Attenuation data for neutrinos with different path-lengths in the Earth carry information about the matter density distribution in the Earth interior. The absorption method of Earth tomography with accelerator neutrino beams, which is difficult (if not impossible) to realise in practice was discussed first in [9,10] and later in grater detail in [11–23].

The oscillations between the active flavour neutrinos and antineutrinos, $\nu_\alpha \leftrightarrow \nu_\beta$ and $\bar{\nu}_\alpha \leftrightarrow \bar{\nu}_\beta$, $\alpha, \beta = e, \mu$ having energies in the range $E \sim (0.1\text{–}15.0)$ GeV and traversing the Earth can be strongly modified by the Earth matter effects (see, e.g., [25]). These modifications depend on the Earth matter density (more precisely, the electron number density $N_e(r)$, see further) along the path of the neutrinos. Thus, by studying the effects of Earth matter on the oscillations of, e.g., ν_μ and ν_e ($\bar{\nu}_\mu$ and $\bar{\nu}_e$) neutrinos traversing the Earth along different trajectories it is possible to obtain information about the Earth (electron number) density distribution.

Atmospheric neutrinos (see, e.g., [26]) are a perfect tool for performing Earth tomography. Consisting of significant fluxes of muon and electron neutrinos and antineutrinos, ν_μ, ν_e, $\bar{\nu}_\mu$ and $\bar{\nu}_e$, produced in the interactions of cosmic rays with the Earth atmosphere, they have a wide range of energies spanning the interval from a few MeV to multi-GeV to multi-TeV. Being produced isotropically in the upper part of the Earth atmosphere at a height of $\sim$ 15 km, they travel distances from $\sim$ 15 km to 12,742 km before reaching detectors located on the Earth surface, crossing the Earth along all possible directions and thus "scanning" the Earth interior. The interaction rates that allow to get information about the Earth density distribution can be obtained in the currently taking data IceCube experiment [27–29] and in the future experiments PINGU [30,31], ORCA [32], Hyper Kamiokande [33,34] and DUNE [35], which are under construction.

The idea of using the absorption method of Earth tomography with atmospheric neutrinos was discussed first, to our knowledge, in [24]. In 2018 in [36] the authors used the data of the IceCube experiment on multi-TeV atmospheric ν_μ and $\bar{\nu}_\mu$ with sufficiently long paths in the Earth and obtained information about the Earth density distribution, which, although not very precise, broadly agrees with the PREM model. More specifically, in [36] it is assumed that the Earth density distribution is spherically symmetric. The analysis is performed with a five layer Earth model: the inner core, two equal width layers of the outer core and two equal width layers of the mantle. The densities in each of the five layers are varied independently. The external constraints on the Earth total mass which is known with a remarkable high precision [37–39], was not applied. The results are obtained with the IceCube data on the zenith angle dependence of the fluxes of up-going atmospheric ν_μ and $\bar{\nu}_\mu$ producing muons with energies in the interval $E_\mu = (0.4\text{–}20.0)$ TeV [40]. Four different models of the initial fluxes of atmospheric ν_μ and $\bar{\nu}_\mu$ were used in the analysis. The value of the Earth mass found in [36], $M^\nu_\oplus = (6.0^{+1.6}_{-1.3}) \times 10^{24}$ kg, is in good agreement with gravitationally determined value [37,38], $M_\oplus = (5.9722 \pm 0.0006) \times 10^{24}$ kg. Thus, the Earth was "weighted" with neutrinos. The results obtained in [36] contain evidence at 2σ C.L. that the core is denser than the mantle: $\bar{\rho}^\nu_c(3\text{layer}) - \bar{\rho}^\nu_{man}(2\text{layer}) = (13.1^{+5.8}_{-6.3})$ g/cm^3, where $\bar{\rho}^\nu_c(3\text{layer})$ and $\bar{\rho}^\nu_{man}(2\text{layer})$ are the values of the average core and mantle densities determined in [36]. This was the first time the study of neutrinos traversing the Earth provided information of the Earth interior and marked the beginning of real experimental data driven neutrino tomography of the Earth.

The Earth tomography based on the study of the effects of Earth matter on the oscillations of atmospheric neutrinos with different path-lengths in the Earth is discussed in [41–43]. In [41] the sensitivity of PINGU and ORCA experiments to the radial density distribution of the Earth has been investigated. The analysis is performed by dividing the PREM density distribution in seven layers as a function of the radial distance d from the Earth surface: 1. Crust, $0 \lesssim d \lesssim 35$ km; 2. Lower Lithosphere, 35 km $\lesssim d \lesssim 60$ km; 3. Upper Mesosphere, 60 km $\lesssim d \lesssim 410$ km; 4. Transition zone, 410 km $\lesssim d \lesssim 660$ km; 5. Lower Mesosphere, 660 km $\lesssim d \lesssim 2860$ km; 6. Outer Core, 2860 km $\lesssim d \lesssim 5151$ km; 7. Inner Core, 5151 km $\lesssim d \lesssim 6371$ km. The layers 2, 3, 4 and 5 correspond to the mantle in PREM. The oscillation probabilities are evaluated by dividing further the layers into certain number of shells with constant densities chosen to match the PREM average densities in each of the shells and by using the evolution operator method (see, e.g., [44]). In the analysis the densities in each layer are varied independently. The constraints of the Earth total mass was not taken into account. Thus, some of the independent variations of the densities in the layers performed in the analysis violate this constraint. The azimuth-averaged ("solar-minimum") $\nu_{e,\mu}$ and $\bar{\nu}_{e,\mu}$ atmospheric neutrino fluxes are taken from [45] and correspond for PINGU and ORCA to the South Pole and Gran Sasso sites. The detection characteristics and the simulation of events in PINGU and ORCA are based respectively

on Refs. [30] and [46,47]. The best fit oscillation parameters and their respective uncertainties are taken from [48]. The results are obtained by the χ^2-minimisation method (for further details of the analysis see [41]). It is found in [41] that using neutrino oscillations it is impossible to get information with the PINGU and ORCA set-ups about the densities in the Crust, Lower Lithosphere and the Inner Core, while the information about the densities of the Upper Mesosphere and the Transitions zone is very imprecise. For example, the density in the Transition zone can be determined with ORCA with 1σ uncertainty of $-$ 61.2%/+ 35.6% ($-$ 52.7%/+ 45.8%) for neutrino mass spectrum with normal (inverted) ordering (NO (IO) spectrum). The sensitivity of PINGU and ORCA to the densities of the Lower Mesosphere $\tilde{\rho}_{\rm LM}$ and the Outer Core $\tilde{\rho}_{\rm OC}$, is found to be significantly higher. In the case of NO (IO) spectrum, $\tilde{\rho}_{\rm LM}$ and $\tilde{\rho}_{\rm OC}$ can be determined, e.g., with ORCA, according to [41], with 1σ uncertainties respectively of $\pm$4% ($-$ 4.7%/+ 4.8%) and $-$ 5.4%/+ 6.0% ($-$ 6.5%/+ 7.1%).

In [42] the authors have analysed the angular and energy distributions of the events in the ORCA detector with the aim of obtaining information on the composition of the Earth core. They conclude, in particular, that for NO (IO) spectrum, after ten years of operation of ORCA the average electron number density in the mantle and in the outer core, for which radial distribution is assumed, can be determined with a precision of $\pm$ 3.6% ($\pm$ 4.6%) and $\pm$ 7.4% ($\pm$ 10.0%) at 1σ C.L. These results are obtained accounting only for the statistical errors of the measurements. In addition, the Earth total mass constraint was not taken into account when varying the density of the mantle or of the outer core.

The possibility to obtain evidence for the existence of the Earth's denser core using the atmospheric neutrino data from the future planned Iron Calorimeter (ICAL) detector at the India-based Neutrino Observatory [49] was studied in [43]. The authors assume, following the PREM model, that the average core density is larger than the average mantle density by a factor $\sim$ 2.5. The results obtained in [43] show, in particular, that using prospective 10 year ICAL data, the simple two-layered mantle-crust Earth density profile can be disfavored with a median χ^2 of 7.45 (4.83) if the case of NO (IO) neutrino mass spectrum, which would provide additional neutrino evidence for the existence of the Earth's denser core.

In the somewhat related studies [50–52] the authors have analysed the IceCube sensitivity to the Earth matter effects in oscillations of atmospheric neutrinos [50] and the IceCube [51] and ORCA [52] sensitivities to the Earth core composition. In [51,52] the PREM density distribution of the Earth core was used as input in the corresponding analyses.

Estimates of the sensitivity to the Earth core density of large $\sim$ 1 Mt (SuperKamiokande-like) water Cerenkov and $\sim$ 100 Kt liquid argon (LAr) detectors using atmospheric neutrino oscillation data were made in [53]. For the PINGU detector similar estimates was made in [54]. A brief account of the studies performed in [53,54] and the results obtained therein is given in Appendix A.

Using PREM as a reference model for the Earth density distribution we investigate in the present article the sensitivity of the ORCA detector to deviations of the Earth (i) outer core (OC) density, (ii) inner core (IC) density, (iii) total core density, and (iv) mantle density, from their respective PREM densities. We consider the case when the radial dependence of the densities of the layers of interest, $\rho_i(r)$, i = IC, OC, core, mantle, is given by PREM and the deviations correspond to an overall scaling factor, i.e., have the form $\rho_i'(r) = (1+\kappa_i)\rho_i(r)$, where κ_i is a real positive or negative constant. The change of density in each Earth layer (IC, OC and mantle) as described by PREM is taken effectively into account, i.e., we do not use the constant density approximation in the layers and shells. The analysis is performed by studying the effects of the Earth matter on the oscillations of atmospheric ν_μ, ν_e, $\bar{\nu}_\mu$ and $\bar{\nu}_e$. For the unoscillated fluxes of the atmospheric neutrinos we use the updated azimuth-averaged energy and zenith angle dependent fluxes from [55] at the Frejus cite.[1] The type of light neutrino mass spectrum is assumed to be known and we obtain results for both the NO and IO spectra. The relevant detection characteristics of the ORCA set-up – the energy and angular resolutions, the dependence of the effective volumes for the different classes of events on the initial neutrino energy, the prospective systematic uncertainties, etc. are taken from the the ORCA proposal [32]. In our analysis we take into account also a number of potential systematic uncertainties identified in [56] and [2] we show the dependence of the results on the type of systematic uncertainties used in the respective analysis. In what concerns the statistical errors, our results correspond to 10 years of operation of ORCA.

Determining the sensitivity of ORCA to the densities of the different Earth structures (or layers) requires to vary the density of a given structure (layer) with respect to its PREM density. Such variation can be incompatible with the total Earth mass value. In order to avoid this in our analysis we systematically implement the total Earth mass constraint. This is done by compensating the variation of the density in a given structure or layer by a corresponding change of the density in one of the other structures or layers. For example, when we vary the OC density, we compensate it by a corresponding variation of the (i) IC density, and of the (ii) mantle density,

[1] In [41] the atmospheric neutrino fluxes from [45] at the Gran Sasso cite, which is more distant from the ORCA location than the Frejus cite, were used.

[2] The study of ORCA sensitivity to the Earth density structure was performed in [41] prior to the publication of the ORCA proposal [32] and, as a consequence, with less systematic error sources than those used in the present work.

so that the total Earth mass constraint is always satisfied. In order to assess the effects of this constraint we present also results without imposing it.[3]

The paper is organised as follows. In Sect. 2 we discuss the basic ingredients of the analysis performed by us, including the PREM input used, the calculation of the relevant neutrino oscillation probabilities, the implementation of the Earth mass constraint and the simulation of events in ORCA. In Sect. 3 we report our results on the sensitivity of ORCA to the IC, OC and mantle densities in the cases of NO and IO neutrino mass spectra. A summary and the conclusions of our work are presented in Sect. 4. Appendix A contains a brief account of the studies performed in [53,54] and the results obtained therein.

2 Basics of the analysis

2.1 PREM input and calculation of oscillation probabilities

We use the PREM model as a reference model of the Earth density distribution $\rho_{\rm E}(r)$ and assume that the location of the mantle-core and the outer core-inner core boundaries are correctly described by the model. Compared to seismic waves, which are usually reflected or refracted at density jumps, neutrino oscillations are essentially not sensitive to changes of density in the Earth mantle and core taking place over distances which are smaller than the neutrino oscillation length [57] (see also [25]) that in the cases we are going to study is typically $\sim$ 1000 km.[4] Thus, they are sensitive, in general, to the average densities of the mantle (or layers of the mantle having width $\sim$ 1000 km), and of the inner core and the outer core (or possibly of two layers of the outer core each having width $\sim$ 1000 km). However, through the mantle-core interference (or neutrino oscillation length resonance- (NOLR-) like) effect [58–60] (see also [61–63] and references quoted therein), the neutrino oscillations are sensitive to the difference of the densities of the mantle and the core, i.e., to the magnitude of the density "jump" in the mantle-core narrow transition zone. They might be sensitive also to the difference between the IC and OC (average) densities.

Some of our results will be obtained by assuming that the density distribution in the mantle, which is known with a relatively good precision [7], is correctly described by the PREM model. We recall that, according to the PREM model, the Earth core has a radius of $R_c = 3480$ km, the IC has a radius of $R_{\rm IC} = 1221.5$ km and OC extends radially from $R_{\rm IC} = 1221.5$ km to $R_{\rm C} = 3480$ km, so the OC radial width is 2258.5 km. The Earth mantle depth is 2856 km. The mean densities of the mantle and the core are respectively $\bar{\rho}_{man} = 4.45$ g/cm^3 and $\bar{\rho}_c = 10.99$ g/cm^3, while the mean densities of the IC and OC are $\bar{\rho}_{\rm IC} = 12.89$ g/cm^3 and $\bar{\rho}_{\rm OC} = 10.90$ g/cm^3.

For a spherically symmetric Earth density distribution, the neutrino trajectory in the Earth is specified by the value of the nadir angle θ_n of the trajectory. For $\theta_n \leq 33.17^o$, or path lengths $L \geq 10{,}665.7$ km, neutrinos cross the Earth core. The path length for neutrinos which cross only the Earth mantle is given by $L = 2R_\oplus \cos\theta_n$. If neutrinos cross the Earth core, the lengths of the paths in the mantle, $2L^{\rm man}$, and in the core, $L^{\rm core}$, are determined by: $L^{\rm man} = R_\oplus \cos\theta_n - (R_c^2 - R_\oplus^2 \sin^2\theta_n)^{\frac{1}{2}}$, $L^{\rm core} = 2(R_c^2 - R_\oplus^2 \sin^2\theta_n)^{\frac{1}{2}}$. Correspondingly, the neutrinos cross the core, the inner core and the outer core for $\cos\theta_n$ lying respectively in the intervals [0.84,1.00], [0.98,1.00] and [0.98,0.84] (the corresponding intervals in θ_n read [0,33.17°], [0,10.98°] and [10.98°,33.17°]).

The Earth matter effects in the neutrino oscillations of interest depend on the matter potential [64–67]

$$V = \sqrt{2}\, G_{\rm F}\, N_e, \tag{1}$$

which involves the electron number density N_e along the path of the neutrinos. The relation between the Earth density and electron number density includes the electron fraction number Y_e (or Z/A factor) of the corresponding Earth structure or layer: $N_e^{(E)}(r) = \rho_{\rm E}(r)\, Y_e/m_{\rm N}$, where $m_{\rm N}$ is the nucleon mass. For isotopically symmetric matter $Y_e = 0.5$. However, the compositions of the Earth mantle and core are not exactly isotopically symmetric. For the outer core, for example, different composition models give a value of Y_e in the interval $Y_e^{oc} = 0.466$–0.471 (see, e.g., [3,68–71]). The value of Y_e in the mantle is closer to 0.5 [3,8]: $Y_e^{man} = 0.490$–0.496. In this study we will use the following default values of Y_e in the mantle and the core: $Y_e^{man} = 0.490$ and $Y_e^{c} = 0.467$.[5]

As is well known, for NO (IO) neutrino mass spectrum, the matter effects can lead to strong enhancement of the neutrino (antineutrino) transition probabilities of interest $P(\nu_\alpha \to \nu_\beta) \equiv P_{\alpha\beta}$ and $P(\bar{\nu}_\alpha \to \bar{\nu}_\beta) \equiv \bar{P}_{\alpha\beta}$, $\alpha \neq \beta = e, \mu$, and $\alpha = e$, $\beta = \tau$, for neutrino energies $E \sim$ (6–10) GeV and $\sim$ (3–5) GeV, corresponding respectively to the resonance in the mantle [64,65,72] (see also [66]) and to the mantle-core interference (NOLR) effect [58]. Although most of the Earth density dependent effects are contained in the energy interval $E \sim$ (2–10) GeV, we will perform our analysis in a large energy interval, $E =$ (2–100) GeV, since, in particular, due to the not very good ORCA energy resolution at low

[3] As the author of [41] indicates, the total Earth mass constraint was not implemented in the analysis performed in [41]. This implies that at least some of the cases of independent variation of the densities in the six layers considered in [41] are unphysical.

[4] The estimate we quote refers to the relevant quantity, $L_{\rm osc}/(2\pi)$, $L_{\rm osc}$ being the neutrino oscillation length.

[5] The relative density deviations from the PREM reference densities to which ORCA may be sensitive we are going to derive do not depend on the specific choices of Y_e^{man} and Y_e^{c} (see further).

energies (see further), the matter effects can appear above 10 GeV in the reconstructed neutrino energy.

For the unoscillated fluxes of atmospheric ν_μ, ν_e, and $\bar{\nu}_\mu$, $\bar{\nu}_e$, $\Phi_\alpha(\theta_n, E)$ and $\bar{\Phi}_\alpha(\theta_n, E)$, we use azimuth-averaged double differential $d^2\Phi_\alpha/(d\cos\theta_n dE)$ and $d^2\bar{\Phi}_\alpha/(d\cos\theta_n dE)$ updated fluxes from [55] [6] at the Frejus cite which is close to the ORCA site. The "source" of atmospheric neutrinos is assumed to be a layer located at 15 km above the Earth surface.

The energy spectra and nadir angle dependencies of the fluxes of atmospheric neutrinos crossing the Earth before reaching the detector are modified by the neutrino oscillation probabilities $P_{\alpha\beta}$ and $\bar{P}_{\alpha\beta}$, $\alpha = e, \mu$, $\beta = e, \mu, \tau$. The Earth is divided into five principal shells: inner core, outer core, lower mantle, transition zone, and upper mantle. The radial distances where there is a transition between the lower mantle and transition zone, and the transition zone and upper mantle are at 5714.8 km and 6014.2 km, respectively. For sub-horizon trajectories ($\theta_n < 90°$), the effects of Earth matter on $P_{\alpha\beta}$ and $\bar{P}_{\alpha\beta}$ are calculated up to the second order in Magnus expansion in each Earth shell as described in [73]. The variation of density in each of the five shells is described by a bi-quadratic polynomial as was done in [73–75]. The coefficients in these polynomials are fixed by the requirement to reproduce in the corresponding shell the variation of density in the PREM model. Thus, the change of density in each shell as described by PREM is taken into account, i.e., we do not use the constant density approximation in the shells.

The oscillation probabilities of interest $P_{\alpha\beta}$ and $\bar{P}_{\alpha\beta}$ depend on all the oscillation parameters $\Delta m^2_{31(23)}$, Δm^2_{21} $\sin^2\theta_{12}$, $\sin^2\theta_{13}$, $\sin^2\theta_{23}$ and δ, where $\Delta m^2_{31(23)}$ corresponds to NO (IO) neutrino mass spectrum, and δ is the Dirac CP violation phase (see, e.g., [25]). In our analysis we use the following reference (true) input values of $\Delta m^2_{31(23)}$, Δm^2_{21} $\sin^2\theta_{12}$, $\sin^2\theta_{13}$ and δ [76]:[7]

$$\Delta m^2_{31(23)} = 2.50 \times 10^{-3}\,\text{eV}^2, \tag{2}$$

$$\Delta m^2_{21} = 7.54 \times 10^{-5}\text{eV}^2, \quad \sin^2\theta_{12} = 0.308, \tag{3}$$

$$\sin^2\theta_{13} = 0.0215, \quad \delta = 3\pi/2. \tag{4}$$

For neutrino energies of interest the probabilities $P_{\alpha\beta}$ and $\bar{P}_{\alpha\beta}$ exhibit rather strong dependence on θ_{23} [61,78–80] (see also [25]). This parameter and the CP violation (CPV) phase δ are still determined in the global analyses of the neutrino oscillation data with a relatively large uncertainty (see, e.g., [76,77]). In the statistical analysis we perform we vary the true value of $\sin^2\theta_{23}$ in the range $\sin^2\theta_{23} \in [0.4, 0.6]$. The test value of $\sin^2\theta_{23}$ is left free in the interval $[0, 1]$, without any external prior. The true value of δ is fixed at $3\pi/2$, but its test value is left free in the interval $[0, 2\pi]$, also without any external prior. The effects of the deviations of the test values of $\Delta m^2_{31(23)}$ and $\sin^2\theta_{13}$ from their true values are taken into account through the pull method [81], assuming the 1σ uncertainties reported in [76]. These uncertainties are somewhat larger than those reported in the latest global data analysis in [77], but this does not have a significant effect on our results. The test values of Δm^2_{21} and $\sin^2\theta_{12}$ are kept fixed at their true values. The analysis is performed assuming that the type of neutrino mass spectrum – with normal ordering or with inverted ordering – is known.

2.2 Total Earth mass constraint

In order to estimate the sensitivity of the ORCA detector to the IC, OC, core (IC + OC) and mantle densities, we vary the density in each of these four structures. We do this variation in one structure at a time and implement the total Earth mass constraint by compensating that variation by corresponding change of the density in one of the other structures. To be more specific, the total Earth mass in the case of interest is given by:

$$\begin{aligned} M_\oplus &= \int_0^{R_\oplus} 4\pi\rho_{\rm E}(r)r^2dr \\ &= 4\pi\left[\int_0^{R_{\rm IC}} \rho_{\rm IC}(r)r^2dr + \int_{R_{\rm IC}}^{R_{\rm C}} \rho_{\rm OC}(r)r^2dr \right. \\ &\quad \left. + \int_{R_{\rm C}}^{R_\oplus} \rho_{\rm man}(r)r^2dr\right], \end{aligned} \tag{5}$$

where $\rho_{\rm IC}(r)$, $\rho_{\rm OC}(r)$ and $\rho_{\rm mant}(r)$ are the IC, OC and mantle densities as a function of r and $R_{\rm IC}$, $R_{\rm C}$ and $R_\oplus$ were defined and their values given earlier. For simplicity we did not indicate in Eq. (5) the division of the mantle in three layers we employ. As we have discussed, the variation of density in each of the five layers we consider (IC, OC and the three mantle layers) is parametrised by bi-quadratic polynomials in such a way as to reproduce the change of density in the PREM model. When we change the density in a given layer $\rho_i(r)$, i = IC, OC, man, by a factor $(1 + \kappa_i)$, where κ_i is r-independent real constant, it means that we multiply the corresponding density distribution by the same factor: $\rho_i(r) \to (1+\kappa_i)\rho_i(r)$. We will present results on sensitivity of ORCA to $\Delta\rho_i = 100\%\,((1 + \kappa_i)\rho_i(r) - \rho_i(r))/\rho_i(r) = 100\%\,\kappa_i$. It follows from Eq. (5) that when we increase (decrease) the density in one layer, in order to keep $M_\oplus$ unchanged, we have to decrease (increase) the density in one of the two, or in both, other layers. The factor by which that has to be done depends on the relative volumes of the layers.

[6] More precisely, we use the "solar minimum, without mountain over the detector" fluxes at the Frejus cite from the tables given in the web site quoted in [55].

[7] The reference values we use are compatible within 1σ C.L. with the best fit values obtained in the latest global analysis in [77].

The approach thus described in the preceding paragraph is implemented in our analysis. When we consider the variation of IC density $\rho_{\rm IC}(r)$, we study two cases: we compensate it by the corresponding change of density of i) the outer core $\rho_{\rm OC}(r)$, and ii) of the mantle $\rho_{\rm man}(r)$. We proceed in a similar way when we analyse the sensitivity of ORCA to the OC and mantle densities $\rho_{\rm OC}(r)$ and $\rho_{\rm man}(r)$: in these two cases we investigate respectively two and three ways of compensating the variation of the respective densities - by the change of $\rho_{\rm IC}(r)$ or of $\rho_{\rm man}(r)$, and by the change of $\rho_{\rm IC}(r)$ or of $\rho_{\rm OC}(r)$ or else of $\rho_{\rm IC}(r)+\rho_{\rm OC}(r) = \rho_{\rm C}(r)$. We consider also the sensitivity of ORCA to the core density $\rho_{\rm C}(r)$. In this case the variation of $\rho_{\rm C}(r)$ is compensated by the change of $\rho_{\rm man}(r)$. In order to assess the effect of the Earth total mass constraint we obtained results on the ORCA's sensitivity to the mantle, outer core, inner core and total core densities without imposing this external constraint.

The method of implementing the total Earth mass constraint using the average IO, OC, core and mantle densities, although less precise, gives quite similar results. We give an example of how the method we employ works by varying the average OC density and compensating this variation with a change of the average mantle density. The average densities of the mantle and the outer core are $\bar{\rho}_{man} = 4.45$ g/cm^3 and $\bar{\rho}_{\rm OC} = 10.90$ g/cm^3, respectively. The contribution to the mass of the Earth depends also on the volume of the layer. The ratio between the volume of the mantle and the volume of the outer core is approximately 5.3. Therefore, a change the outer core density by, e.g., 10%, should be compensated with a variation of the mantle density by $10\% \times 10.90/(4.45 \times 5.3) = 4.62\%$.

As we have indicated, the neutrino oscillation probabilities relevant for our analysis depend on the Earth electron number density $N_e^{(E)}$ and not directly on the Earth matter density $\rho_{\rm E}(r)$: $N_e^{(E)}(r) = \rho_{\rm E}(r)\, Y_e/m_{\rm N}$. In our analysis we fixed the electron fraction numbers (or the Z/A factors) of the mantle and the core to the following reference values: $Y_e^{man} = 0.490$ and $Y_e^c = 0.467$. Therefore when we vary $\rho_{\rm IC}(r)$, $\rho_{\rm OC}(r)$ $\rho_{\rm C}(r)$ and $\rho_{\rm man}(r)$ we vary the electron number densities in these layers, $N_e^{(i)}(r)$, $i = {\rm IC, OC, C, man}$. For any fixed value of Y_e^i of a given layer, the quantity $\Delta\rho_i$ we will determine statistically from prospective ORCA data does not depend on Y_e^i. As a consequence we have: $\Delta\rho_i = 100\%\,((1+\kappa_i)N_e^i(r) - N_e^i(r))/N_e^i(r) = \Delta N_e^{(i)}$, i.e., our results on sensitivity of ORCA to $\Delta\rho_i$ are also results on sensitivity of ORCA to deviations of the electron number densities of the different Earth layers from their PREM reference values.

We note also that the uncertainties in the values of Y_e^{man} and Y_e^c [3,68–70] induce uncertainties in the sensitivity of ORCA to the IC, OC, core and mantle matter densities which are much smaller than those due to the combination of statistical and systematic errors in the ORCA data. For this reason we did not take them into account.

2.3 Simulation of events in ORCA

We calculate the principal observables in ORCA detector – the double differential event spectra in the neutrino energy E and nadir angle θ_n using the methods developed and described in [56,75]. We comment briefly on some of the technical aspects of the calculations.

The neutrino events in ORCA are divided into two classes [32]: "track-like" and "cascade-like". Track-like events involve an outgoing μ^- or μ^+ and originate from charged current (CC) interactions of ν_μ, $\bar{\nu}_\mu$ and ν_τ, $\bar{\nu}_\tau$. Cascade-like events result from CC interactions of ν_e, $\bar{\nu}_e$ and ν_τ, $\bar{\nu}_\tau$, and from neutral current interactions and consist of hadronic and electromagnetic showers.

The ORCA "Letter of Intent" [32] contains estimates of the probabilities of flavour-misidentification as well as of identifying the τ and the neutral current events as track or cascade events. We include this information from [32] in our analysis.

The relevant detection characteristics of ORCA – the energy and angular resolutions and the dependence of the effective volumes for the different types/classes of events on the initial neutrino energy - are taken from [32] and correspond to the benchmark (9 m vertical spacing) configuration of the ORCA experiment. Note that in [32] such characteristics are only provided in graphical form, whereas the analytical formulas that have been implemented in our code, as well as the relevant factors, are obtained through private communication with the experimental collaboration, as it also happened in [56], where one of the authors of this work was involved.

In our analysis we consider $E \in [2, 100]$ GeV and $\theta_n/\pi \in [0, 0.5]$. These two ranges are divided into 20 equally-spaced bins (linearly for θ_n and logarithmically for E), for a total of 400 bins for cascade events and an equal number for track events.

The statistical analysis of ORCA event distributions is performed employing the χ^2 method described in [75]. In the analysis we include, in addition to the statistical uncertainties, the following systematic uncertainties [56]:

1. oscillation and normalization uncertainties, where the latter include an overall normalization error (15%), as well as the relative μ/e and $\nu/\bar{\nu}$ flux uncertainties (8% and 5%, respectively);
2. energy-scale (5%) and energy-angle resolution uncertainties (10%), independently for cascade and track events;
3. energy-angle spectral shape uncertainties, via quartic polynomials in both θ_n and E. These are meant to char-

acterize systematic effects including: uncertainties in the primary cosmic ray fluxes, differential atmospheric neutrino fluxes and cross sections and, to some extent, energy-angle detection efficiencies;
4. residual uncorrelated systematics in each bin, representing the presence of unknown uncertainties, like those coming from a finite Monte Carlo statistics in experimental simulations.

We define as "minimal" set of systematics the one including only those described in point (1) in the preceding list. When we add the uncertainties at point (2), (3) and (4), assuming a prior of 0.75% (1.5%) on the coefficients of the quartic polynomials and a 0.75% (1.5%) uncorrellated error in each bin, we obtain our "optimistic" set ("default" set). Finally, if we instead consider a 3% uncertainty on polynomial coefficients and uncorrelated errors we get our "conservative" set. All the systematics mentioned above are implemented using the pull method [81].

3 Results

In the next five subsections we present the results of our analysis on the sensitivity of ORCA to the (i) OC density $\rho_{\rm OC}(r)$, (ii) IC density $\rho_{\rm OC}(r)$, (iii) total core density $\rho_{\rm core}(r)$ and (iv) mantle density $\rho_{\rm man}(r)$. In each case we impose the total Earth mass constraint, compensating the variation of the density in a given layer by corresponding changes of density in one of the other layers. In other to assess the effects of this constraint we show also results without imposing it.

To illustrate the dependence of the sensitivity of ORCA on the systematic uncertainties we obtained results for the four types of possible systematic uncertainties, which can affect significantly the sensitivity of ORCA and which are still not well determined: the "minimal", "optimistic", "default" and "conservative" sets defined earlier. We choose to present results only for the "minimal", "optimistic" and "conservative" sets of uncertainties.

As we have discussed earlier, in the analysis we have performed we kept δ and $\sin^2\theta_{23}$ fixed to certain values. We have obtained results for $\delta = 3\pi/2$ and eleven values of $\sin^2\theta_{23}$ from the interval [0.40, 0.60]. In what follows we present results for three reference values of $\sin^2\theta_{23} = 0.42$, 0.50 and 0.58,[8] which belong to, and essentially span, the 3σ range of allowed values of $\sin^2\theta_{23}$ obtained in the latest global neutrino data analyses [77,82]. All results are obtained assuming 10 years of ORCA operation. In Sects. 3.1–3.4 we present results for NO neutrino mass spectrum. Results for IO spectrum are reported in Sect. 3.5.

One more comment is in order. It follows from the seismological data as well as the condition of hydrostatic equilibrium of the Earth that the following inequalities should always hold:

$$\rho_{man} \leq \rho_{OC} \leq \rho_{IC}. \tag{6}$$

These constraints are not *a priori* satisfied when we vary the density in a given layer and compensate it with a change of density in another layer. However, we indicate in each specific case what are the restrictions they lead to whenever these restrictions are relevant.

3.1 Sensitivity to the Outer Core Density

In the present subsection we show results on the sensitivity of ORCA to the OC density in the cases of mantle and IC being the "compensating" layers and when the total Earth mass constraint is not imposed.

3.1.1 Compensation with Mantle Density

Figure 1 illustrates the sensitivity of ORCA to $\rho_{\rm OC}(r)$ when the Earth total mass constraint is implemented and the OC density variation is compensated with a corresponding mantle density change. The figure shows the χ^2-distribution as a function of the OC relative density variation with respect to the PREM value, $\Delta\rho_{\rm outer\ core}$. The results shown are for $\sin^2\theta_{23} = 0.42$, 0.50, 0.58 (left, center and right panels) and in the cases of "minimal", "optimistic" and "conservative" systematic errors (top, middle and bottom panels). All χ^2-distributions in Fig. 1 have a symmetric, or slightly asymmetric, Gaussian form. As follows from Fig. 1, in the case of "minimal" systematic errors, ORCA can determine the OC density at 3σ with an uncertainty of $(-33\%)/+23\%$, $(-24\%)/+18\%$ and $(-18\%)/+15\%$ respectively for $\sin^2\theta_{23} = 0.42$, 0.50, 0.58. The positive (negative) values correspond to $\Delta\rho_{\rm outer\ core} > 0$ ($\Delta\rho_{\rm outer\ core} < 0$). In the case of "conservative" systematic errors, the sensitivity is noticeably worse: $(-43\%)/+39\%$, $(-37\%)/+30\%$ and $(-30\%)/+24\%$ for $\sin^2\theta_{23} = 0.42$, 0.50, 0.58, respectively. For $\sin^2\theta_{23} = 0.58$ (0.50), the sensitivity is worse approximately by a factor of (1.6–1.7) (of 1.5 (of 1.7) for negative (positive) $\Delta\rho_{\rm outer\ core}$). As could be expected, in the case of "optimistic" systematic errors the sensitivity of ORCA under discussion is somewhat worse (better) than that obtained with "minimal" ("conservative") systematic errors.

Working in the considered case with the average PREM values of $\bar\rho_{man} = 4.45$ g/cm^3, $\bar\rho_{\rm OC} = 10.90$ g/cm^3 and $\bar\rho_{\rm IC} = 12.89$ g/cm^3, it is not difficult to show that the inequalities in Eq. (6) imply approximately $(-49.6\%) \lesssim \Delta\rho_{\rm outer\ core} \lesssim 18.3\%$. In what concerns the derived ORCA

[8] The results for the additional values of $\sin^2\theta_{23}$ are used to assess the effects of the Earth hydrostatic equilibrium conditions on the results derived accounting for the Earth mass constraint (see further).

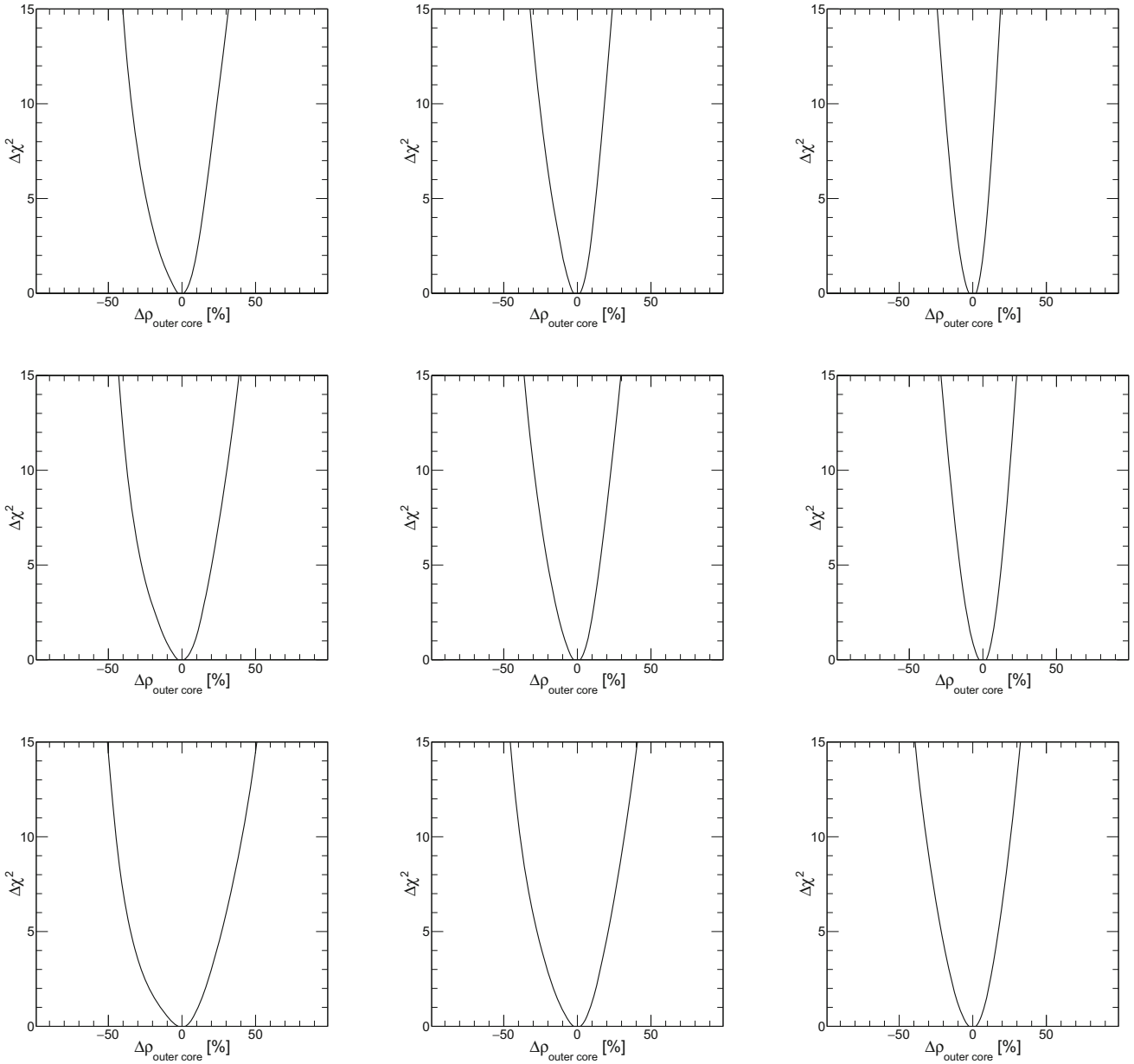

Fig. 1 Sensitivity to the OC density in the case of NO spectrum and 10 years of data. The Earth total mass constraint is implemented by compensating the OC density variation with a corresponding mantle density change. The results shown are for $\sin^2\theta_{23} = 0.42, 0.50, 0.58$ (left, center and right panels) and in the cases of "minimal", "optimistic" and "conservative" systematic errors (top, middle and bottom panels). See text for further details

3σ sensitivity ranges of $\Delta\rho_{\text{outer core}}$, the lower limit from the external constraint (6) has no effect on them. The effect of the upper limit of 18.3% depends on the type of implemented systematic errors and on the value of $\sin^2\theta_{23}$: the smaller the systematic errors and/or the larger $\sin^2\theta_{23}$, the smaller the effect is. In the case of "minimal" systematic errors, the indicated upper limit has no effect on the ORCA 3σ sensitivity ranges for any $\sin^2\theta_{23} \gtrsim 0.50$; for $\sin^2\theta_{23} = 0.42$ it corresponds to the maximal value of the ORCA 2σ sensitivity range. For the set of "optimistic" systematic errors, 18.3% represents approximately the maximal value of the 2σ, 2.4σ and 2.6σ ORCA sensitivity ranges for $\sin^2\theta_{23} = 0.50$, 0.54 and 0.58, respectively. The effect of the discussed constraint is largest for the ranges of interest obtained with conservative systematic errors: 18.3% corresponds, e.g., to the maximal value of the ORCA 1.9σ sensitivity range at $\sin^2\theta_{23} = 0.58$.

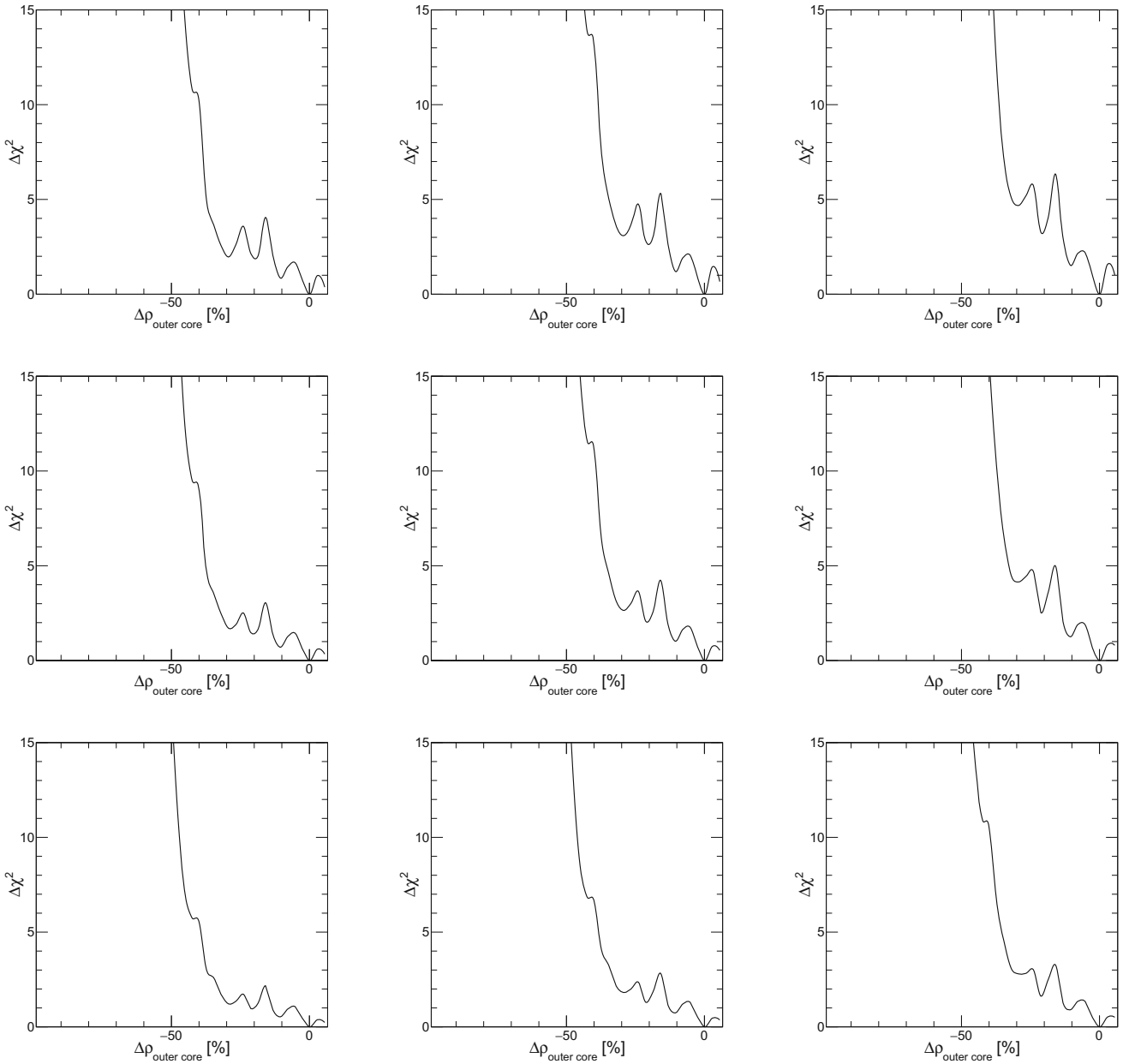

Fig. 2 The same as in Fig. 1, but with the Earth total mass constraint implemented by compensating the OC density variation with a corresponding inner core density change. The results shown are for $\sin^2\theta_{23} = 0.42, 0.50, 0.58$ (left, center and right panels) and in the cases of "minimal", "optimistic" and "conservative" systematic errors (top, middle and bottom panels). See text for further details

3.1.2 Compensation with Inner Core Density

In Fig. 2 we present results on the sensitivity of ORCA to the OC density when the Earth total mass constraint is implemented and the OC density variation is compensated with a corresponding IC density change. All χ^2-distributions shown in Fig. 2 have an asymmetric non-Gaussian form. As Fig. 2 indicates, in this case ORCA is not sensitive to OC densities which are larger than the PREM OC density. This is due, in particular, to the fact that the IC mass is much smaller that the OC mass and only an insignificant increase of the OC density can be compensated by a decrease of the IC density. The wiggles seen in Fig. 2 reflect the dependence of the relevant oscillation probabilities on the correlated modifications of the OC and IC densities. In the case of "minimal" systematic errors and $\Delta\rho_{\text{outer core}} < 0$, ORCA can determine the OC density for $\sin^2\theta_{23} = 0.42, 0.50, 0.58$ with an uncertainty respectively of (-39%), (-37%) and (-35%) at 3σ C.L. In the case of "conservative" systematic errors, the sensitivity reads (-46%), (-45%) and (-38%) for $\sin^2\theta_{23} = 0.42, 0.50,$

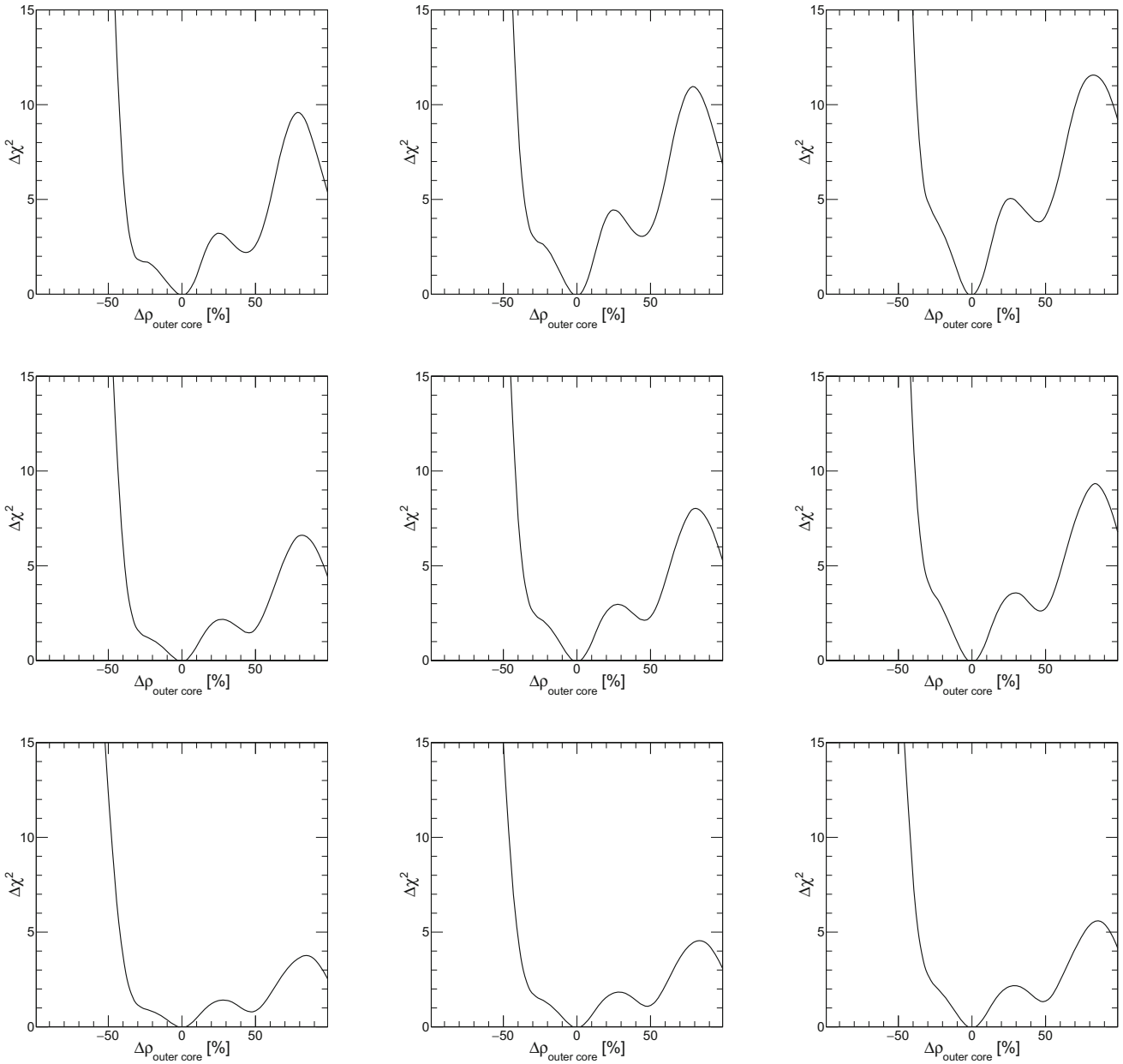

Fig. 3 The same as in Fig. 1, but without implementing the Earth total mass constraint. The results shown are for $\sin^2\theta_{23} = 0.42, 0.50, 0.58$ (left, center and right panels) and in the cases of "minimal", "optimistic" and "conservative" systematic errors (top, middle and bottom panels). See text for further details

0.58, respectively. All these values are bigger than the external constraint (-49.6) $\lesssim \Delta\rho_{\text{outer core}}$ following from Eq. (6). There is a relatively weak dependence on both $\sin^2\theta_{23}$ and the type of the implemented systematic uncertainty within those considered by us. The sensitivity to OC density in this case is much worse than in the case when the mantle is used as a "compensating" layer, considered earlier.

3.1.3 Without compensation

We get very different results on the sensitivity of ORCA to the OC density when the total Earth mass constraint is not implemented. This case is unphysical, except for insignificant deviations of the OC density from the PREM value. The corresponding results are shown in Fig. 3. The χ^2 dependence on $\Delta\rho_{\text{outer core}}$ is asymmetric and non-Gaussian. The sensitivity is, in general, much worse than in the case of enforcing the total Earth mass constraint with mantle being the "compensating" layer. Even in the "most favorable" case

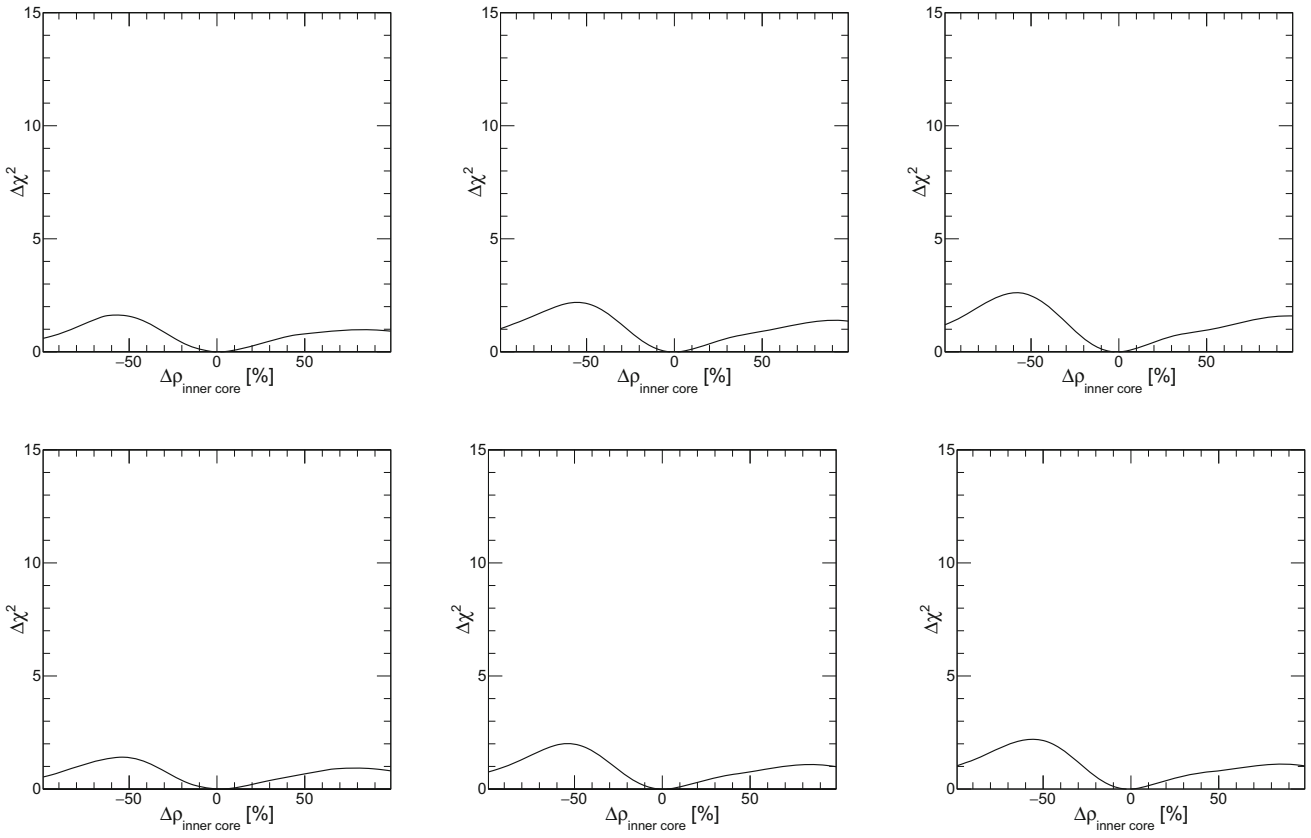

Fig. 4 Sensitivity to the IC density. The Earth total mass constraint (i) is implemented by compensating the IC density variation with a corresponding mantle density change (top panels), (ii) is not implemented (bottom panels). The results shown are for $\sin^2\theta_{23} = 0.42, 0.50, 0.58$ (left, center and right panels) and in the case of "minimal" systematic errors. See text for further details

of "minimal" uncertainties and $\sin^2\theta_{23} = 0.58$, for example, ORCA can be sensitive at 3σ only to relatively large deviations of OC density from the PREM value, which are $\sim 38\%$ for $\Delta\rho_{\text{outer core}} < 0$ and are larger for $\Delta\rho_{\text{outer core}} > 0$.

3.2 Sensitivity to the inner core density

Our results show that ORCA is essentially insensitive to deviations of the IC density from the PREM value, corresponding to $|\Delta\rho_{\text{inner core}}| \leq 100\%$. This conclusion is valid for all values of $\sin^2\theta_{23}$, all possible "compensating" layers and all possible systematic uncertainties considered. Although the IC density is largest in the Earth, the IC volume, as given by PREM, is much smaller than the OC and mantle volumes. As a consequence, the IC contribution to the Earth total mass is also much smaller that the OC and mantle contributions.

The sensitivity of ORCA to the IC density is illustrated in Fig. 4 in the case of "minimal" systematic uncertainties. The top panels are obtained by imposing the Earth total mass constraint and compensating the IC density variation with a corresponding mantle density change, while in the bottom panels we show results derived without implementing this constraint.

3.3 Sensitivity to the core density

In the present subsection we present results on the ORCA prospective sensitivity to the total core density. They are obtained by considering deviations of the IC and OC densities by the same constant scale factor from their respective PREM densities. We consider two cases: (i) compensating the variation of the core density by corresponding change of the mantle density so as to satisfy the total Earth mass constraint, and (ii) not imposing the total Earth mass constraint when varying the total core density.

3.3.1 Compensation with mantle density

Figure 5 illustrates the sensitivity of ORCA to the total core density $\rho_C(r)$ when the "compensating" layer is the mantle. In the figure, the χ^2-distribution is shown as a function of the core relative density variation with respect to the PREM value, $\Delta\rho_{\text{core}}$. As in the other considered cases, the reported

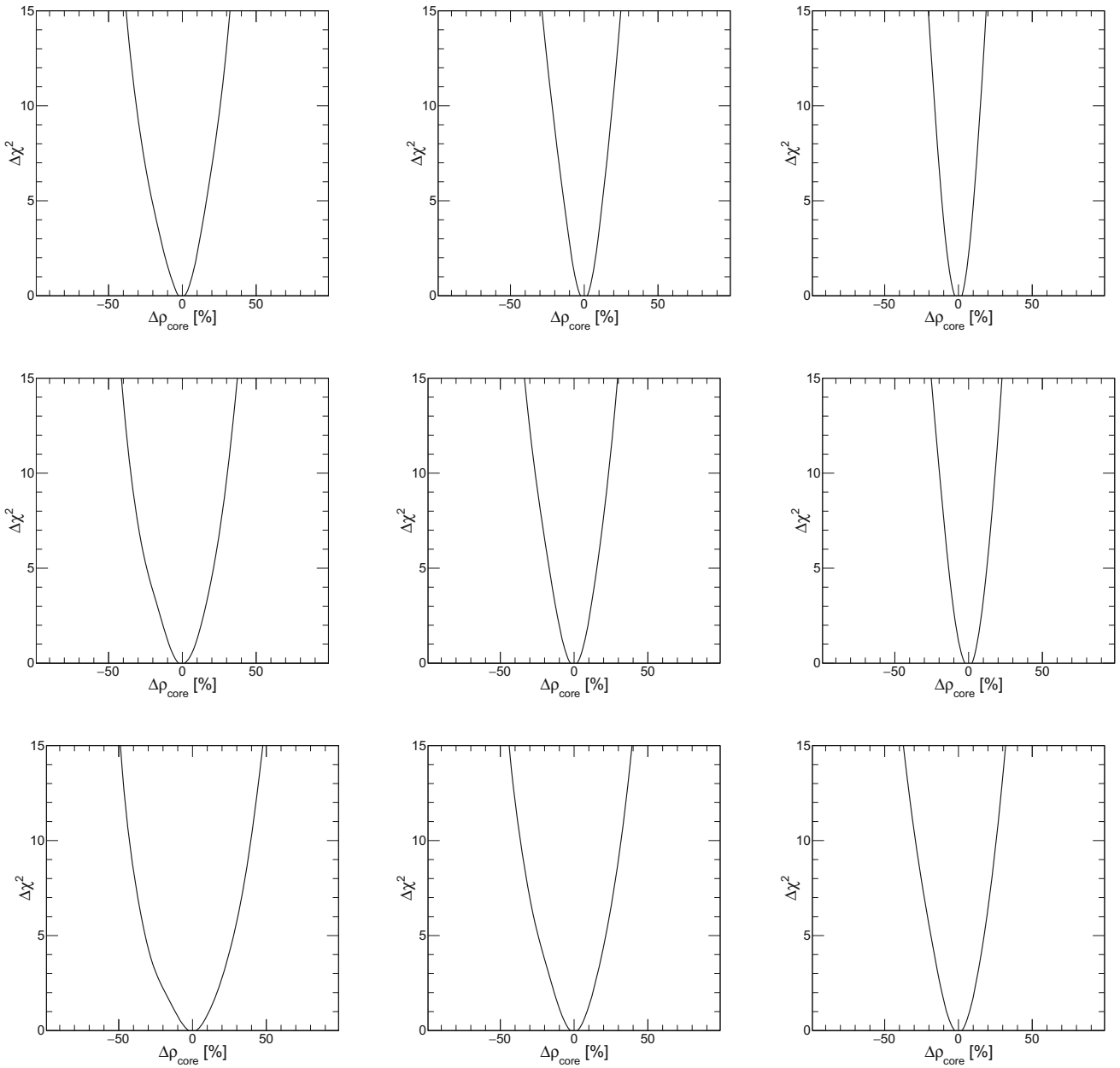

Fig. 5 Sensitivity to the core density in the case of NO spectrum and 10 years of data. The Earth total mass constraint is implemented by compensating the core density variation with a corresponding mantle density change. The results shown are for $\sin^2\theta_{23} = 0.42, 0.50, 0.58$ (left, center and right panels) and in the cases of "minimal", "optimistic" and "conservative" systematic errors (top, middle and bottom panels). See text for further details

results are for $\sin^2\theta_{23} = 0.42, 0.50, 0.58$ (left, center and right panels) and in the cases of "minimal", "optimistic" and "conservative" systematic errors (top, middle and bottom panels).

According to our results, the sensitivity of ORCA to $\Delta\rho_{\text{core}}$ for the three types of systematic errors considered are similar to, or somewhat better than, the results on ORCA sensitivity to $\Delta\rho_{\text{outer core}}$ when OC density change is compensated by mantle density change, reported in Fig. 1. All χ^2-distributions in Fig. 5 have a symmetric or slightly asymmetric Gaussian form. In the case of "minimal" systematic errors, ORCA can determined the core density at 3σ with an uncertainty of $(-\ 29\%)/+\ 24\%$, $(-\ 20\%)/+\ 18\%$ and $(-\ 15\%)/+\ 15\%$ respectively for $\sin^2\theta_{23} = 0.42, 0.50, 0.58$. In the case of "conservative" systematic errors, the sensitivity reads: $(-\ 40\%)/+\ 38\%$, $(-\ 35\%/+\ 30\%$ and $(-\ 28\%)/+\ 24\%$ for $\sin^2\theta_{23} = 0.42, 0.50, 0.58$, respectively. For $\sin^2\theta_{23} = 0.58$

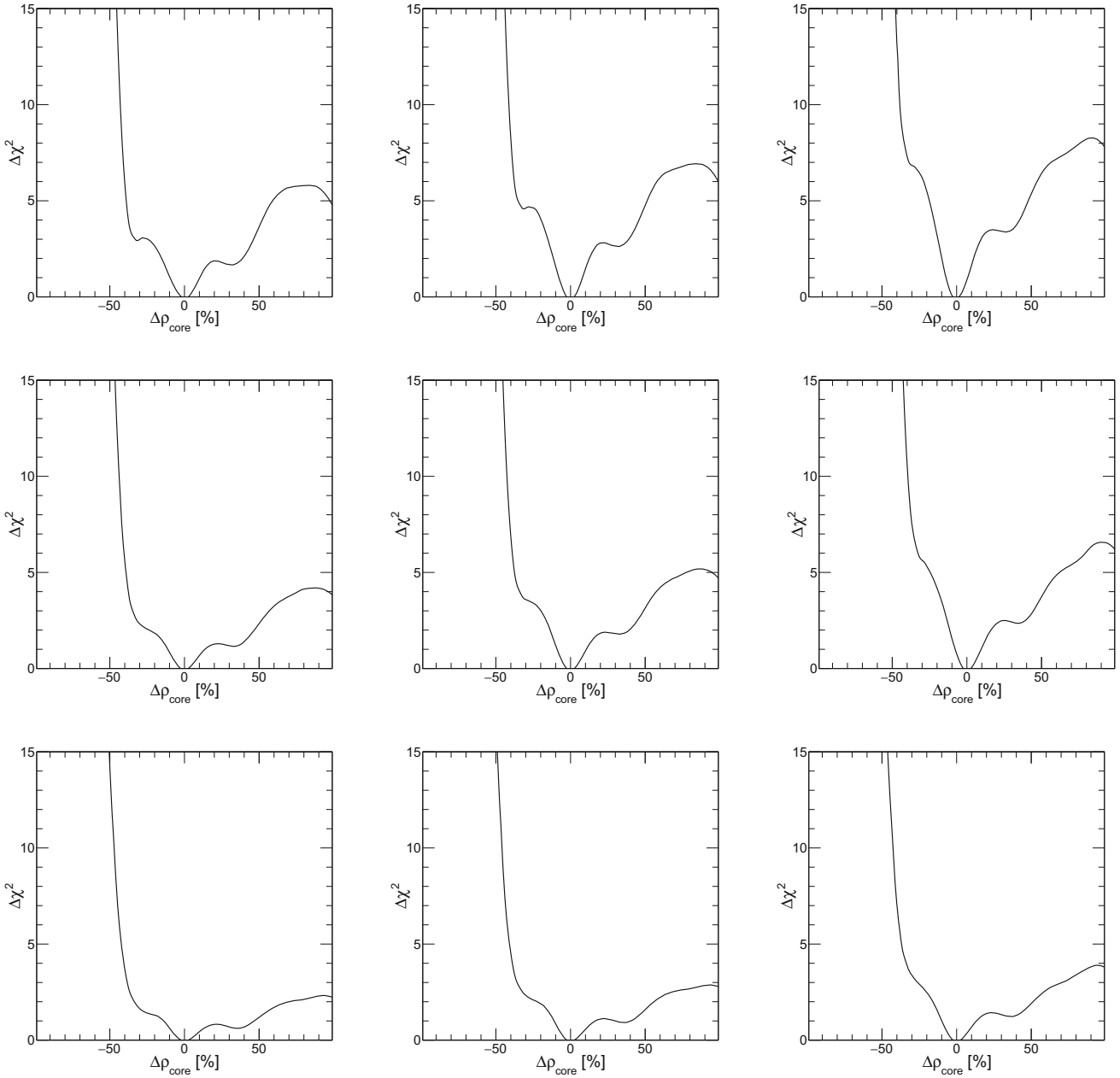

Fig. 6 The same as in Fig. 5, but without implementing the Earth total mass constraint. The results shown are for $\sin^2\theta_{23} = 0.42, 0.50, 0.58$ (left, center and right panels) and in the cases of "minimal", "optimistic" and "conservative" systematic errors (top, middle and bottom panels). See text for further details

(0.50), it is worse by a factor of $\sim$ (1.6–1.9) than the sensitivity corresponding to "minimal" systematic errors.

The constraint $\rho_{man} \leq \rho_{core}$ implies maximal negative $\Delta\rho_{core}$ of (-57%), which has no effect on the 3σ maximal negative variation of ρ_{OC} to which ORCA might be sensitive.[9]

[9] Adding the Earth moment of inertia constraint, would fix (up to the uncertaities in the constraints) the values of ρ_{man} and ρ_{core}. This case will be considered elsewhere.

3.3.2 Without compensation

The sensitivity of ORCA to the core density when the total Earth mass constraint is not implemented is similar to that of the OC density under the same conditions (see Fig. 3). The results corresponding to this case are presented in Fig. 6. The χ^2 distributions shown in Fig. 6 as a function of $\Delta\rho_{\rm core}$ are asymmetric and non-Gaussian. Compared to the case of enforcing the total Earth mass constraint with mantle being the "compensating" layer, the sensitivity is much worse. It

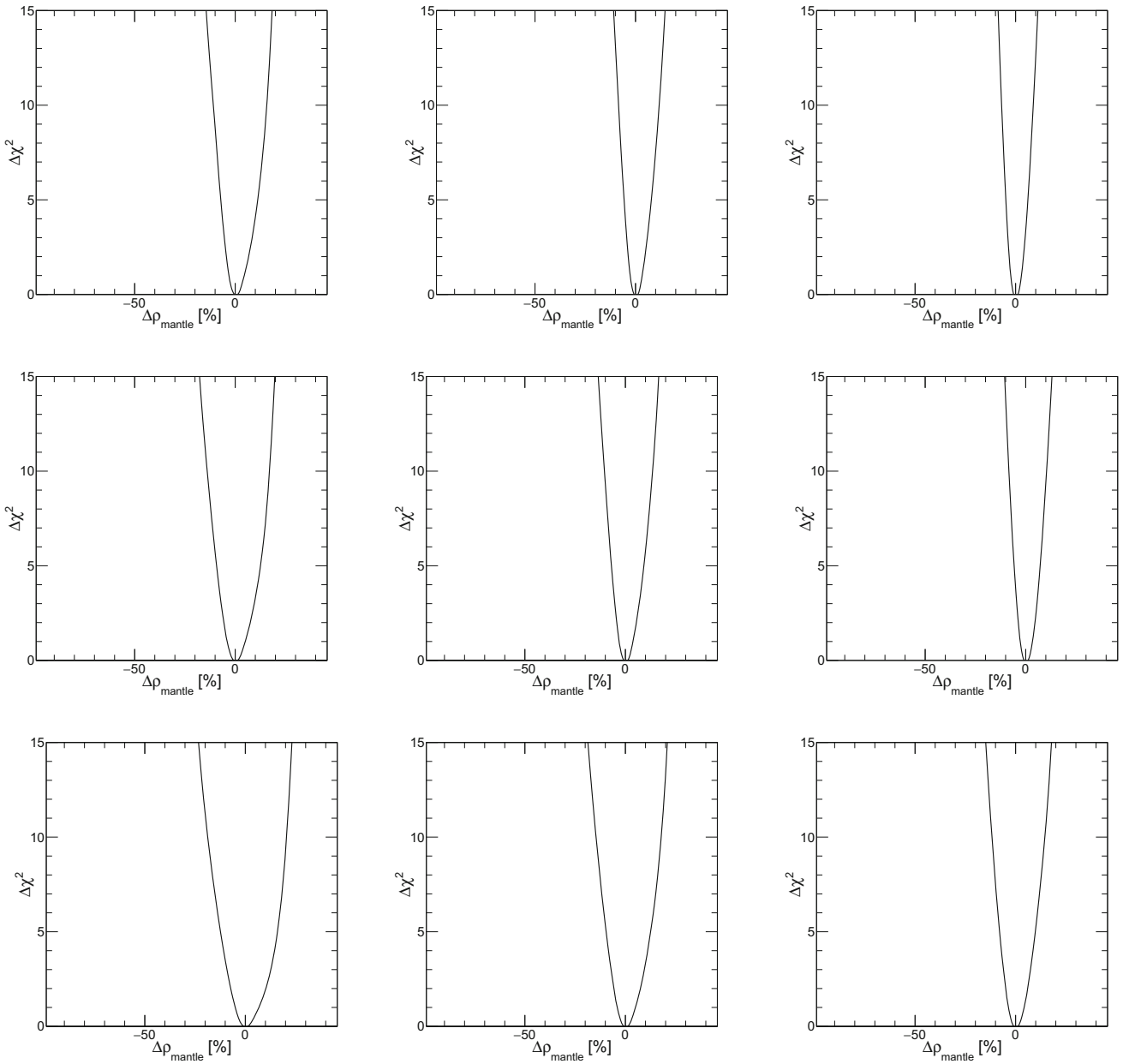

Fig. 7 Sensitivity to the mantle density in the case of NO spectrum and 10 years of data. The Earth total mass constraint is implemented by compensating the mantle density variation with a corresponding OC density change. The results shown are for $\sin^2\theta_{23} = 0.42, 0.50, 0.58$ (left, center and right panels) and in the cases of "minimal", "optimistic" and "conservative" systematic errors (top, middle and bottom panels). See text for further details

follows from Fig. 6, in particular, that for $\sin^2\theta_{23} = 0.58$ and "minimal" systematic uncertainties, which are the "most favorable" conditions ensuring the highest sensitivity, ORCA can be sensitive at 3σ C.L. only to relatively large deviations of the core density from that given by PREM, namely, to $\sim 38\%$ for $\Delta\rho_{\text{core}} < 0$ and to much larger deviations for $\Delta\rho_{\text{core}} > 0$.

3.4 Sensitivity to the mantle density

3.4.1 Compensation with outer core density

Our results show that ORCA will have rather high sensitivity to the Earth mantle density if OC (or total Earth core) is used as a compensation layer when imposing the total Earth mass constraint. They are presented graphically in Fig. 7 in which we show χ^2 versus $\Delta\rho_{\text{mantle}}$ with OC being the compensating

layer. The results correspond, as in the previous cases, to $\sin^2\theta_{23} = 0.42, 0.50, 0.58$ (left, center and right panels) and "minimal", "optimistic" and "conservative" systematic errors (top, middle and bottom panels).

The χ^2 dependence on $\Delta\rho_{\rm mantle}$ in Fig. 7 has symmetric or slightly asymmetric Gaussian form. As follows from Fig. 7, ORCA can determine the mantle density 3σ with an uncertainty of $(-11\%)/+13\%$, $(-9\%)/+11\%$ and $(-6\%)/+8\%$ for $\sin^2\theta_{23} = 0.42, 0.50, 0.58$, respectively, and "minimal" systematic errors. The sensitivity of ORCA is somewhat worse in the case of "conservative" systematic errors: for $\sin^2\theta_{23} = 0.42, 0.50, 0.58$ the uncertainties of interest are given at 3σ C.L. respectively by $(-17\%)/+20\%$, $(-13\%/+17\%$ and $(-11\%)/+14\%$, implying still a relatively high ORCA sensitivity to $\rho_{\rm man}$. Depending on the value of $\sin^2\theta_{23}$, the uncertainties are larger than those corresponding to "minimal" systematic errors approximately by factors of $\sim$ (1.4–1.8). We find that for "optimistic" systematic errors the uncertainty under discussion for $\sin^2\theta_{23} = 0.42, 0.50, 0.58$ at 3σ C.L. reads, respectively: $(-14\%)/+17\%$, $(-10\%)/+13\%$ and $(-8\%)/+10\%$. As can be expected, it is somewhat larger (smaller) than the ORCA uncertainty corresponding to "minimal" ("conservative") systematic errors.

As can be shown, the conditions in Eq. (6) imply $(-8.3\%) \lesssim \Delta\rho_{mantle} \lesssim 22.8\%$. These conditions do not restrict from above the the ORCA 3σ sensitivity range of $\Delta\rho_{\rm mantle} > 0$ even in the case of "conservative" systematic errors. The maximal negative variation of $\Delta\rho_{\rm mantle}$ of (-8.3%) restricts from below the ORCA sensitivity ranges derived employing the Earth mass constraint, the smaller the systematic erors and/or the larger $\sin^2\theta_{23}$, the smaller the effect of the external condition $\Delta\rho_{\rm mantle} \gtrsim -8.3\%$ is. In the case of "minimal" systematic errors, $\Delta\rho_{\rm mantle} = -8.3\%$ corresponds to the minimal values of the ORCA 2σ, 2.4σ, 2.8σ and 3.0σ sensitivity ranges derived for $\sin^2\theta_{23} = 0.46$, 0.50, 0.54 and 0.58, respectively. With implemented "optimistic" systematic errors, it coincides with the minimal values of the ORCA 2.0σ, 2.4σ and 2.7σ sensitivity ranges for $\sin^2\theta_{23} = 0.48$, 0.54 and 0.58. And in the case of "conservative" systematic errors, it is equal to the minimal value of the 2.0σ sensitivity range for $\sin^2\theta_{23} = 0.58$.

With maximally reduced systematic errors and certain further improvements (e.g., the discussed "favorable" 6 m vertical spacing configuration of ORCA experiment [32] or the Super-ORCA version of the detector [83]) the ORCA sensitivity to negative $\Delta\rho_{\rm mantle}$ might increase sufficiently so that the external constraints $(-8.3\%) \lesssim \Delta\rho_{\rm mantle}$ would have no effect on the ORCA 3σ sensitivity to negative $\Delta\rho_{\rm mantle}$.

3.4.2 Compensation with inner core density

We get quite different results when IC is used as a "compensating" layer. They are presented in Fig. 8. The sensitivity of ORCA to $\rho_{\rm man}$ is still very high for $\Delta\rho_{\rm mantle} < 0$. For $\Delta\rho_{\rm mantle} > 0$ ORCA practically is not sensitive to $\rho_{\rm man}$. As in the similar case of variation of $\rho_{\rm OC}$ compensated with a change of $\rho_{\rm IC}$, this is a consequence of the fact that the IC mass is much smaller than the mantle mass and only insignificant increase of the mantle mass can be compensated by decreasing the IC mass.

As Fig. 8 indicates, in the considered case ORCA can determine the mantle density at 3σ C.L. with an uncertainty $\Delta\rho_{\rm mantle}$ of (-14%), (-12%) and (-8%) for $\sin^2\theta_{23} = 0.42, 0.50, 0.58$, respectively, and "minimal" systematic errors. The sensitivity of ORCA in the case of "conservative" systematic errors and $\sin^2\theta_{23} = 0.42, 0.50, 0.58$ corresponds at 3σ C.L. respectively to $\Delta\rho_{\rm mantle}$ of (-22%), (-18%) and (-14%). We find that for "optimistic" systematic errors the uncertainty under discussion for $\sin^2\theta_{23} = 0.42$, 0.50, 0.58 at 3σ C.L. reads, respectively: (-16%), (-14%) and (-9%).

3.4.3 Without compensation

The sensitivity of ORCA to the mantle density $\rho_{\rm man}$ when the total Earth mass constraint is not imposed is significantly worse than in the case of imposing it and OC is used as a compensating layer. The results corresponding to this case are reported graphically in Fig. 9. The χ^2 dependence on $\Delta\rho_{\rm mantle}$ in Fig. 9 has somewhat asymmetric Gaussian form. According to Fig. 9, ORCA can determine the mantle density at 3σ C.L. when the total Earth mass constraint is not implemented with an uncertainty $\Delta\rho_{\rm mantle}$ of $(-14\%)/+20\%$, $(-11\%)/+17\%$ and $(-9\%)/+12\%$ for $\sin^2\theta_{23} = 0.42, 0.50, 0.58$, respectively, and "minimal" systematic errors. In case of "optimistic" and "conservative" systematic errors we get for $\sin^2\theta_{23} = 0.42, 0.50, 0.58$ respectively $(-17\%)/+24\%$, $(-13\%)/+18\%$, $(-10\%)/+13\%$ and $(-22\%)/+36\%$, $(-18\%)/+25\%$, $(-14\%)/+18\%$. Depending on the value of $\sin^2\theta_{23}$, the 3σ uncertainty in $\rho_{\rm mantle}$ in the case of "conservative" systematic errors is larger than that for "minimal" systematic errors by a factor of $\sim$ (1.5–1.8).

3.5 Results for IO neutrino mass spectrum

We have performed exactly the same analysis ("minimal", "optimistic", "default" and "conservative" sets of systematic errors, eleven values of $\sin^2\theta_{23}$ from the interval [0.40, 060], $\delta = 3\pi/2$, implementing the total Earth mass constraint and not imposing it) assuming IO neutrino mass spectrum. In all cases considered we find that the sensitivity of ORCA detector to deviations of the densities of the different Earth structures (IC, OC, core, mantle) from their respective PREM reference values is significantly worse than that in the case of NO neutrino mass spectrum. This is essentially due to the fact that for the IO spectrum only the antineutrino oscillation

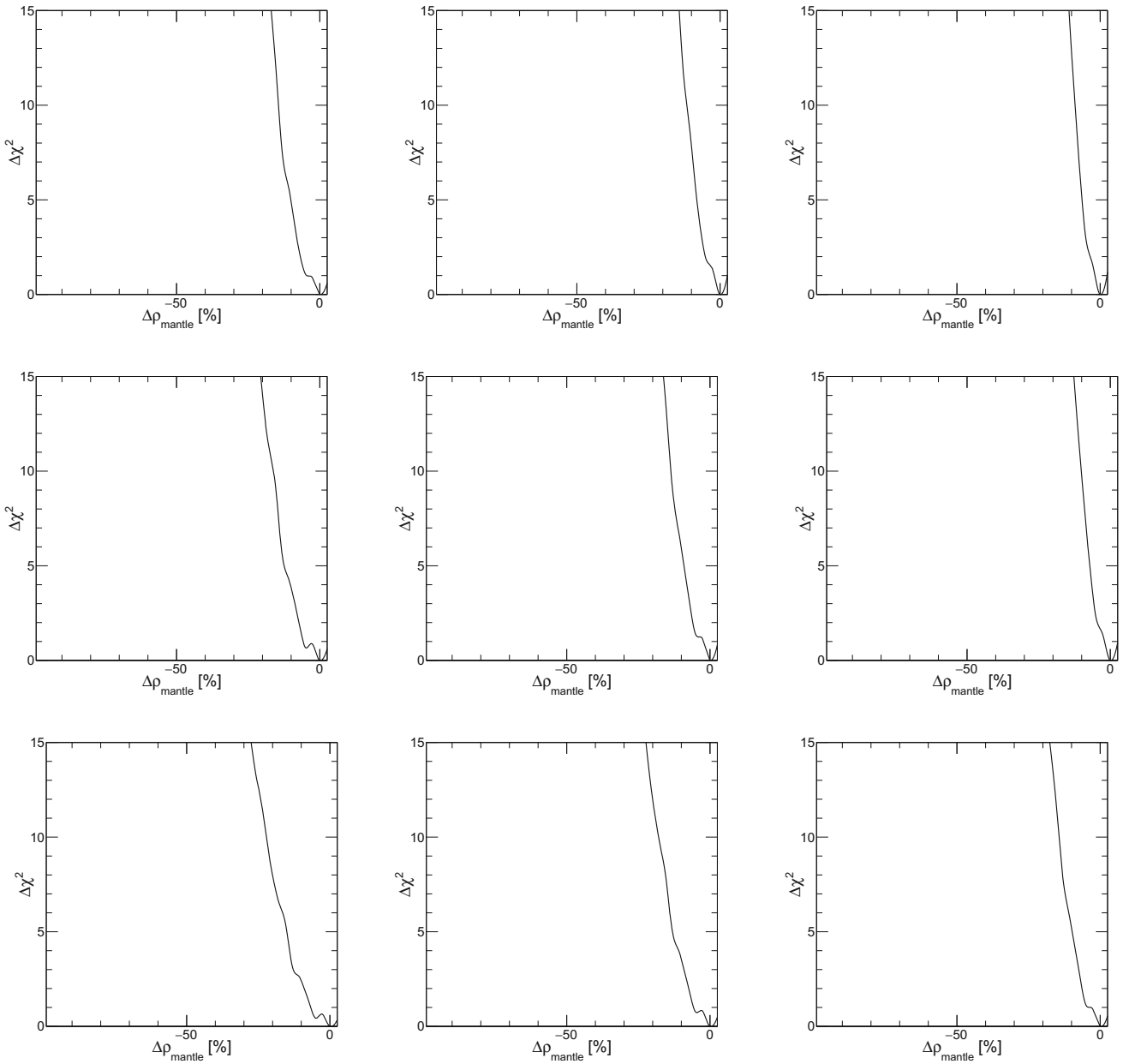

Fig. 8 The same as in Fig. 7, but with implementing the Earth total mass constraint by compensating the mantle density variation with a corresponding IC density change. The results shown are for $\sin^2\theta_{23} = 0.42, 0.50, 0.58$ (left, center and right panels) and in the cases of "minimal", "optimistic" and "conservative" systematic errors (top, middle and bottom panels). See text for further details

probabilities $\bar{P}_{\alpha\beta}$, $\alpha = e, \mu$, $\beta = e, \mu, \tau$, can be amplified by the matter effects, while for the energies of interest the anti-neutrino cross sections are approximately by a factor of two smaller than the neutrino cross sections. In view of the above we present below only selected illustrative minimal subset of our results for the IO spectrum.

In Fig. 10 we present results on sensitivity of ORCA to the OC and total core densities with mantle being the "compensating" layer. The results shown are for $\sin^2\theta_{23} = 0.42, 0.50, 0.58$ (left, center and right panels). The panels in the first two rows (last two rows) in Fig. 10 illustrate the sensitivity to the OC (core) density and are obtained using "minimal" (1st and 3rd row panels) and "optimistic" (2nd and 4th row panels) sets of systematic errors. The χ^2-distributions in in Fig. 10 have symmetric or slightly asymmetric Gaussian form.

In the case of most favorable "minimal" systematic error set, our results show that for $\sin^2\theta_{23} = 0.42, 0.50, 0.58$, ORCA can determine the OC (core) density at 3σ C.L. with uncertainties of $\mp 45\%$, $\mp 37\%$ and $\mp 30\%$ ($(-40\%)/+44\%$, $(-32\%)/+36\%$ and $(-25\%)/+30\%$), respectively. For the

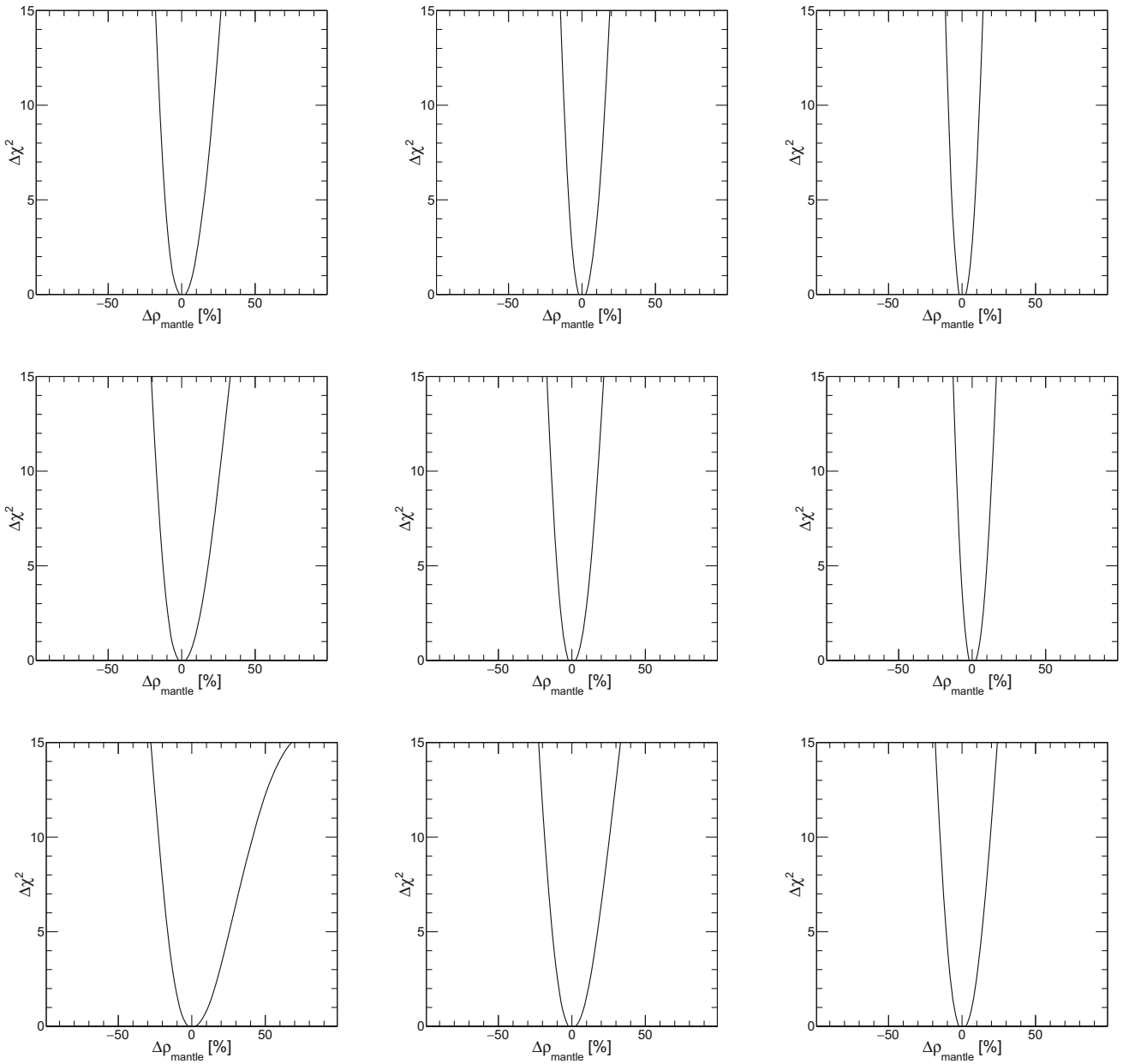

Fig. 9 The same as in Fig. 7, but without implementing the Earth total mass constraint. The results shown are for $\sin^2\theta_{23} = 0.42, 0.50, 0.58$ (left, center and right panels) and in the cases of "minimal", "optimistic" and "conservative" systematic errors (top, middle and bottom panels). See text for further details

"optimistic" and "conservative" sets of errors we get respectively for the indicated three values of $\sin^2\theta_{23}$: (− 47%)/+ 52%, (− 38%)/+ 42%, (− 33%)/+ 34%, and (− 63%)/+ 70%, (− 52%)/+ 57%, (− 47%)/+ 48% ((− 44%)/+ 50%, (− 36%)/+ 40%, (− 30%)/+ 33%), and ((− 58%)/+ 57%, (− 50%)/+ 53% and (− 43%)/+ 45%)).[10] They should be compared with the corresponding results for the NO spectrum reported in Figs. 1 and 5. It follows form this comparison, in particular, that in the case of IO spectrum the ORCA sensitivity to the OC and core densities is worse than the sensitivity in the case of NO spectrum by factors that can be as large as ~ 2.5.

4 Summary and conclusions

In the present article we have investigated the sensitivity of the ORCA detector to deviations of the Earth (i) outer core (OC) density, (ii) inner core (IC) density, (iii) total core den-

[10] The results for the "conservative" set of errors are not shown in Fig. 10. We quote them here for completeness.

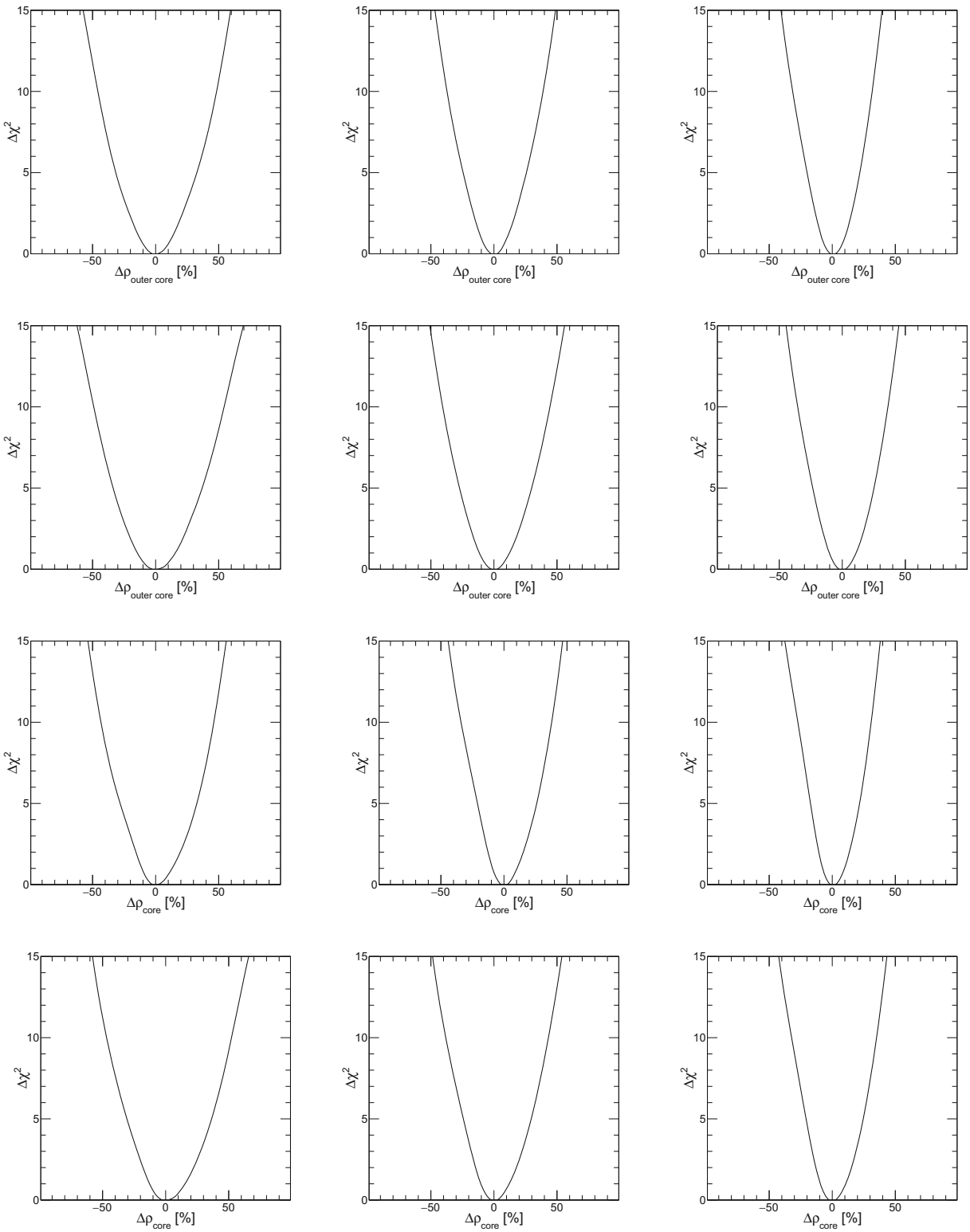

Fig. 10 Sensitivity to the OC (1st and 2nd row panels) and core (3rd and 4th row panels) densities in the case of IO spectrum and 10 years of data. The Earth total mass constraint is implemented by compensating the variations of the OC and core densities with corresponding mantle density changes. The results shown are for $\sin^2\theta_{23} = 0.42, 0.50, 0.58$ (left, center and right panels) and in the cases of "minimal" (1st and 3rd row panels) and "optimistic" (2nd and 4th row panels) sets of errors. See text for further details

sity, and (iv) mantle density, from their respective PREM reference densities. We have considered the case when the radial dependence of the densities of the layers of interest, $\rho_i(r)$, i = IC, OC, core, mantle, is given by PREM and the deviations correspond to an overall scaling factor, i.e., have the form $\rho_i'(r) = (1+\kappa_i)\rho_i(r)$, where κ_i is a real positive or negative constant. The results we present on sensitivity of ORCA are for the relative deviations of the densities $\rho_i(r)$ from their PREM reference values, i.e., for $100\%(\rho_i'(r)-\rho_i(r))/\rho_i(r) = 100\%\kappa_i$. The change of density in each Earth layer (IC, OC and mantle) as described by PREM was taken effectively into account, i.e., we did not use the constant density approximation in the considered layers and shells. The analysis was performed by studying the effects of the Earth matter on the oscillations of atmospheric ν_μ, ν_e, $\bar{\nu}_\mu$ and $\bar{\nu}_e$. The relevant neutrino oscillation probabilities depend on the electron number densities of the Earth layers of interest, $N_e^{(i)}$: $N_e^{(i)}(r) = Y_e^{(i)}\rho_i(r)/m_{\rm N}$, where $Y_e^{(i)}$ is the electron fraction number (or the Z/A factor) of the layer i = IC, OC, core, mantle. In the analysis we have performed we have set Y_e of the mantle and the core to fixed values, $Y_e^{man} = 0.490$ and $Y_e^{c} = 0.467$. Thus, when we vary the matter density $\rho_{\rm i}(r)$, i = IC, OC, C, man, we actually vary the electron number density of the corresponding layer, $N_e^{(i)}(r)$, i = IC, OC, C, man. As a consequence the results on sensitivity of ORCA to the matter densities of the different Earth structures are results on sensitivity of ORCA to the electron number densities of these Earth structures. They do not depend on the chosen fixed values of Y_e^{man} and Y_e^{c}.

For the unoscillated fluxes of the atmospheric neutrinos we used the azimuth-averaged energy and zenith angle dependent fluxes from [55] at the Frejus cite. We assumed that the type of light neutrino mass spectrum is known and we obtain results for both the NO and IO spectra. The relevant detection characteristics of the ORCA set-up – the energy and angular resolutions, the dependence of the effective volumes for the different classes of events on the initial neutrino energy, the prospective systematic uncertainties, etc. were taken form the the ORCA proposal [32]. We took into account also a number of potential systematic uncertainties identified in [56] and studied the dependence of the results on the type of systematic uncertainties used. The statistical errors employed in our analysis correspond to 10 years of operation of ORCA.

In determining the sensitivity of ORCA to the densities of the different Earth layers, which requires to consider deviations of the density of a given layer from its PREM reference density, we systematically implemented the constraint following the precise knowledge of the total Earth mass. This was done by compensating the variation of the density in the considered layer by a corresponding change of the density in one of the other layers.

More specifically, when we consider the variation of IC density $\rho_{\rm IC}(r)$, we studied two cases: compensating it by the corresponding change of density of (i) the outer core $\rho_{\rm OC}(r)$, and (ii) of the mantle $\rho_{\rm man}(r)$. We proceeded in a similar way when we analyse the sensitivity of ORCA to the OC and mantle densities $\rho_{\rm OC}(r)$ and $\rho_{\rm man}(r)$: in these two cases we investigate respectively two and three ways of compensating the variation of the respective densities – by the change of $\rho_{\rm IC}(r)$ or of $\rho_{\rm man}(r)$, and by the change of $\rho_{\rm IC}(r)$ or of $\rho_{\rm OC}(r)$ or else of $\rho_{\rm IC}(r)+\rho_{\rm OC}(r) = \rho_{\rm C}(r)$. We considered also the sensitivity of ORCA to the core density $\rho_{\rm C}(r)$. In this case the variation of $\rho_{\rm C}(r)$ is compensated by the change of $\rho_{\rm man}(r)$. In order to asses the effects of the total Earth mass constraint we presented also results without imposing it.

Following the described procedure we have derived and reported results on the sensitivity of ORCA to the (i) OC density $\rho_{\rm OC}(r)$, (ii) IC density $\rho_{\rm OC}(r)$, (iii) total core density $\rho_{\rm core}(r)$ and iv) mantle density $\rho_{\rm man}(r)$. We have derived results for four different sets of systematic uncertainties which can affect significantly the sensitivity of ORCA, "minimal", "optimistic", "default" and "conservative" (defined in Sect. 2). To illustrate the dependence of the sensitivity of ORCA on the systematic uncertainties and not burden the presentation, we presented results only for "minimal", "optimistic" and "conservative" sets of uncertainties.

In the analysis we have performed we kept the Dirac phase δ and $\sin^2\theta_{23}$ fixed to certain values and assumed that mass spectrum of light neutrinos, which can be with normal ordering (NO) or inverted ordering (IO) is known. We have obtained results for $\delta = 3\pi/2$, eleven values of $\sin^2\theta_{23}$ from the interval [0.40, 0.60] and the two types of neutrino mass spectrum. Rather detailed results were presented only for three reference values of $\sin^2\theta_{23} = 0.42$, 0.50 and 0.58, which belong to, and essentially span, the 3σ range of allowed values of $\sin^2\theta_{23}$ obtained in the latest global neutrino data analyses [77,82], and for NO spectrum (Sects. 3.1–3.4). We reported also results obtained assuming IO neutrino mass spectrum (Sect. 3.5).

In our analysis the Earth hydrostatic equilibrium constraints given in Eq. (6) are not *a priori* satisfied when we vary the density in a given layer and compensate it with a change of density in another layer. However, we indicated in each specific case what are the restrictions they lead to whenever these restrictions are relevant. In general, in the cases when they are relevant the smaller the systematic errors and/or the larger $\sin^2\theta_{23}$, the smaller the effect of the constraints is.

Our results show that the ORCA detector in the configuration considered in KM3NeT 2.0 LoI for ORCA [32], which we used in our analysis, is practically not sensitive to the IC density. We find further that that the sensitivity of ORCA to the densities of the outer core, core and mantle depend strongly

1. on the value of $\sin^2\theta_{23}$,
2. on the type of systematic errors employed in the analysis,

3. on whether the total Earth mass constraint is implemented or not, and
4. on the way the compensation of the density variation in a given layer by a change of density in another layer is implemented, i.e., on the choice of the "compensating" layer, when the total Earth mass constraint is imposed.

It depends also strongly on the type of neutrino mass spectrum.

The sensitivity of ORCA to the outer core (core) and mantle densities is found in our analysis to be highest/maximal

(i) for the largest value of $\sin^2\theta_{23}$ allowed by the data;
(ii) in the case when the total Earth mass constraint is implemented and the variation of the outer core (total core) and mantle densities is compensated by changes respectively of the mantle and outer core or total core densities;
(iii) and, obviously, for the "minimal" or "optimistic" set of systematic errors.

We have shown , in particular, that in the "most favorable" NO case of "minimal" systematic errors, $\sin^2\theta_{23} = 0.58$ and implemented Earth mass constraint as in point ii), ORCA can determine, e.g., the OC (mantle) density at 3σ C.L. after 10 years of operation with an uncertainty of (− 18%)/+ 12% (of (− 6%)/+ 8%). In the "most disfavorable" NO with implemented Earth mass constraint as in point ii) but "conservative" systematic errors and $\sin^2\theta_{23} = 0.42$, the uncertainty reads (− 43%)/+ 39% ((− 17%/+ 20%), while for for $\sin^2\theta_{23} = 0.50$ and 0.58 it is noticeably smaller: (− 37)%/+ 30% and (− 30%)/+ 24% ((− 13%)/+ 17% and (− 11%/+ 14%)).

In the case of OC (mantle) density variation compensated by a change of the mantle (OC) density, the Earth hydrostatic equilibrium constraints, Eq. (6), imply approximately $(-49.6\%) \lesssim \Delta\rho_{\text{outer core}} \lesssim 18.3\%$ $((-8.3\%) \lesssim \Delta\rho_{mantle} \lesssim 22.8\%)$. In what concerns the derived ORCA 3σ sensitivity ranges of $\Delta\rho_{\text{outer core}}$ reported above, (i) the lower limit from the external constraints in Eq. (6) has no effect on them, (ii) the effects of the upper limit of 18.3%, if any, depends on $\sin^2\theta_{23}$ and on the type of implemented systematic errors. More specifically, the upper limit of 18.3% has no effect on the ORCA 3σ sensitivity ranges in the case of "minimal" systematic errors for any $\sin^2\theta_{23} \gtrsim 0.50$; for $\sin^2\theta_{23} = 0.42$, it corresponds to the maximal value of the ORCA 2σ sensitivity range. Fot the set of "optimistic" systematic errors, 18.3% represents approximately the maximal value of the 2σ, 2.4σ and 2.6σ ORCA sensitivity ranges for $\sin^2\theta_{23} = 0.50$, 0.54 and 0.58, respectively. The effect of the discussed constraint is largest for the ORCA sensitivity ranges obtained with conservative systematic errors: 18.3% corresponds, e.g., to the maximal value of the ORCA 1.9σ sensitivity range at $\sin^2\theta_{23} = 0.58$.

In a similar way, the external constraints in Eq. (6) do not restrict from above the reported ORCA 3σ sensitivity to $\Delta\rho_{mantle}$ even in the case of "conservative" systematic errors. The maximal allowed negative variation of (− 8.3%) restricts from below the ORCA sensitivity ranges. More specifically, in the case of "minimal" systematic errors, $\Delta\rho_{\text{mantle}} = -8.3\%$ corresponds to the minimal values of the ORCA 2σ, 2.4σ, 2.8σ and 3.0σ sensitivity ranges derived for $\sin^2\theta_{23} = 0.46$, 0.50, 0.54 and 0.58, respectively. With implemented "optimistic" systematic errors, it coincides with the minimal values of the ORCA 2.0σ, 2.4σ and 2.7σ sensitivity ranges for $\sin^2\theta_{23} = 0.48$, 0.54 and 0.58. And in the case of "conservative" systematic errors, it is equal to the minimal value of the 2.0σ sensitivity range for $\sin^2\theta_{23} = 0.58$.

With maximally reduced systematic errors and certain further improvements, e.g., the discussed "favorable" 6 m vertical spacing configuration of ORCA experiment [32] or the Super-ORCA version of the detector [83], the ORCA sensitivities to positive $\Delta\rho_{\text{outer core}}$ (negative $\Delta\rho_{\text{mantle}}$) might increase sufficiently so that the external constraint $\Delta\rho_{\text{outer core}} \lesssim 18.3\%$ $((-8.3\%) \lesssim \Delta\rho_{\text{mantle}})$ would have no effect on the ORCA 3σ sensitivity to positive variations of ρ_{OC} compensated by changes of ρ_{mantle} (negative variations of ρ_{mantle} compensated by changes of ρ_{OC}).

The uncertainties in the determination of the outer core, total core and mantle densities by ORCA in the case of NO spectrum, according to our results, are considerably larger if the total Earth mass constraint is not implemented in the analysis, or if it is implemented but the inner core is used as a "compensation" layer.

We find also that the sensitivity of ORCA to the outer core, core and mantle densities is significantly worse for the IO neutrino mass spectrum than for the NO spectrum (Fig. 10, Sect. 3.5). In the case of most favorable "minimal" systematic error set our results show, for example, that for $\sin^2\theta_{23} = 0.42$, 0.50, 0.58, ORCA can determine the OC density at 3σ C.L. if mantle is used as a "compensating" layer with uncertainties of $\mp 45\%$, $\mp 37\%$ and $\mp 30\%$, respectively. For the "optimistic" and "conservative" sets of errors we get for the indicated three values of $\sin^2\theta_{23}$: (− 47%)/+ 52%, (− 38%)/+ 42%, (− 33%)/+ 34%, and (− 63%)/+ 70%, (− 52%)/+ 57%, (− 47%)/+ 48%. They should be compared with the corresponding results for the NO spectrum reported in Fig. 1. It follows form this comparison, in particular, that in the case of IO spectrum the ORCA sensitivity to the OC density is worse than the sensitivity in the case of NO spectrum by factors that can be as large as ~ 2.5. We find similarly that the sensitivity of ORCA to the core and mantle densities for IO neutrino mass spectrum are also worse than that in the case of NO spectrum.

On the basis of the results of these study we can conclude that the ORCA experiment has the potential of making unique

pioneering contributions to the studies of the Earth interior with atmospheric neutrinos, i.e., to the neutrino tomography of the Earth.

Note Added. While the text of this article was being written, Refs. [84,85] appeared on the arXiv. In [84] the authors investigated the sensitivity of the DUNE experiment to the Earth core, lower mantle and upper mantle densities by using prospective DUNE data on oscillations of atmospheric neutrinos, while in [85] prospective atmospheric neutrino DUNE data were used with the aim of determining the radius of the Earth core.

Acknowledgements S.T.P. would like to thank S. Choubey for many discussions over the years of various aspects of neutrino tomography of the Earth. This project was supported in part by the European Union's Horizon 2020 research and innovation programme under the Marie Sklodowska-Curie grant agreement no. 860881-HIDDeN, by the Italian INFN program on Theoretical Astroparticle Physics and by the World Premier International Research Center Initiative (WPI Initiative, MEXT), Japan (S.T.P.). The work of F.C. at Virginia Tech is supported by the U.S. Department of Energy under the award grant number DE-SC0020250. The work of F.C. at IFIC (Valencia, Spain) is supported by GVA Grant no. CDEIGENT/2020/003.

Data Availability Statement This manuscript has no associated data or the data will not be deposited. [Authors' comment: The present study is purely theoretical.]

Open Access This article is licensed under a Creative Commons Attribution 4.0 International License, which permits use, sharing, adaptation, distribution and reproduction in any medium or format, as long as you give appropriate credit to the original author(s) and the source, provide a link to the Creative Commons licence, and indicate if changes were made. The images or other third party material in this article are included in the article's Creative Commons licence, unless indicated otherwise in a credit line to the material. If material is not included in the article's Creative Commons licence and your intended use is not permitted by statutory regulation or exceeds the permitted use, you will need to obtain permission directly from the copyright holder. To view a copy of this licence, visit http://creativecommons.org/licenses/by/4.0/.
Funded by SCOAP[3].

Appendix A: Early Preliminary Estimates

In [53] the sensitivities of $\sim$ 1 Mt SuperKamiokande-like water Cerenkov detector and of $\sim$ 100 Kt liquid argon (LAr) detector to the Earth (outer) core density were estimated using prospective atmospheric neutrino oscillation data. The characteristics of the detectors and the methods developed in [86,87] for studies of neutrino mass ordering determination with these detectors were employed in [53].

In the case of the water Cerenkov detector, both e-like and μ-like events produced by atmospheric neutrinos with energy E in the multi-GeV range (2–10) GeV were taken into account. This range was divided into eight bins of equal width of 1 GeV. Three Earth core bins in $\cos\theta_z$, θ_z being the zenith angle, were used: one corresponding to the inner core and two equal width bins corresponding to the outer core. The atmospheric neutrino fluxes from [88] were utilised in the analysis. Following [86], the energy and zenith angle resolution functions were assumed to have Gaussian forms with quite optimistic widths: $\sigma_{\rm E} = 0.10\,E$ (0.05E) and $\Delta\theta_z = 7^\circ$ (5°). Results for the somewhat more realistic values $\sigma_{\rm E} = 0.15E$ and $\Delta\theta_z = 10^\circ$ were also obtained. The neutrino oscillation parameters were fixed to $|\Delta m^2_{31(23)}| = 2.50 \times 10^{-3}\,{\rm eV}^2$, $\Delta m^2_{21} = 8.0 \times 10^{-5}\,{\rm eV}^2$ $\sin^2\theta_{12} = 0.31$, $\sin^2\theta_{23} = 0.50$ and $\delta = 0$. In what concerns $\sin^2 2\theta_{13}$, it was found that maximal sensitivity is obtained for $\sin^2 2\theta_{13} = 0.05$ and this value was used in the study. In the χ^2-analysis only statistical errors corresponding to exposure of 10 Mty were included. The results, e.g., on the outer core density sensitivity were derived by changing the PREM outer core density by an overall fixed scale factor. The inner core and mantle densities were kept fixed at their PREM values. It was found in [53], in particular, that in the case of NO neutrino mass spectrum and $\sigma_{\rm E} = 0.10\,E$ (0.05E) and $\Delta\theta_z = 7^\circ$ (5°), a water Cerenkov detector may have a 2σ C.L. sensitivity to a 20% (15%) outer core density deviation from its PREM density. These results were quite discouraging.

In [53] aspects of atmospheric neutrino oscillation tomography of the Earth with a 100 Kt prototype of LAr detector [89–91] with magnetisation over the detector's volume [92] have been investigated using the characteristics of the detector considered in [87]. The results of this study were not published since the technical characteristics of the proposed LAr detector were evolving continuously (the mass of the detector was reduced, the magnetisation option was abandoned, etc.) and eventually the "realistic" design of the detector differed significantly from that used in the study.

We show graphically in Fig. 11 the results obtained in [54] on PINGU sensitivity to the inner core, outer core and mantle densities for NO spectrum and after 10 years of operation. The PINGU characteristics used in the analysis were taken from [30], while the atmospheric neutrino fluxes are from [45]. Both e-like and μ-like events were included in the study. The total Earth mass constraint was not implemented and only the statistical uncertainties were accounted for in the analysis. The results shown in Fig. 11 were obtained for the following (true) values of the neutrino oscillation parameters: $\Delta m^2_{31(23)} = 2.46\times10^{-3}\,{\rm eV}^2$, $\Delta m^2_{21} = 7.6\times10^{-5}\,{\rm eV}^2$ $\sin^2\theta_{12} = 0.32$, $\sin^2\theta_{23} = 0.50$ and $\delta = 0$. The parameter $\sin^2 2\theta_{13}$ was varied in the interval (0.020–0.025). The sensitivities of interest were calculated with and without marginalisation over $\Delta m^2_{31(23)}$, θ_{23} and θ_{13}. The differences between the two sets of results depend on the deviations from the PREM densities considered but are typically smaller than one unit of the relevant χ^2 function. According to the results obtained in [54] and illustrated graphically in Fig. 11, in the case of NO neutrino mass spectrum, PINGU in the config-

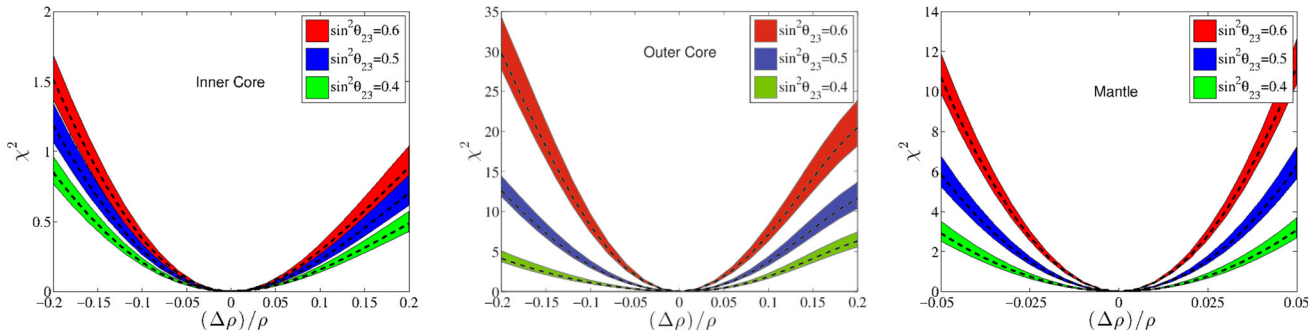

Fig. 11 PINGU prospective sensitivity to the inner core (left panel), outer core (middle panel) and mantle (right panel) densities in the case of NO spectrum and 10 years of data. The ratios $\Delta\rho/\rho$ in the three panels correspond respectively to $\Delta\rho_{\text{inner core}}$, $\Delta\rho_{\text{outer core}}$ and $\Delta\rho_{\text{mantle}}$ defined in the main text. The results shown are for $\sin^2\theta_{23} = 0.40$, 0.50, 0.60. The bands correspond to variation of $\sin^2\theta_{13}$ in the interval 0.020–0.025 and marginalisation over θ_{23}, Δm^2_{31} and θ_{13}. See text for further details. (Figures from [54])

uration proposed in [30] and after 10 years of data-taking will have a rather good sensitivity to the outer core and mantle densities and essentially no sensitivity to the inner core density. More specifically, it follows from Fig. 11, in particular, that for, e.g., $\sin^2\theta_{23} = 0.5$, PINGU may be sensitive at 3σ C.L. to $\Delta\rho_{\text{outer core}} \cong \pm 17\%$ and at 2.5σ C.L. to $\Delta\rho_{\text{mantle}} \cong \pm 5\%$.

References

1. B.A. Bolt, Q. J. R. Astron. Soc. **32**, 367 (1991)
2. C.F. Yoder, in *Global Earth Physics*, vol. 1, ed. by T.J. Ahrens (American Geophysical Union, Washington DC, 1995), p. 1
3. W.F. McDonough, in *Treatise on Geochemistry: The Mantle and Core"*, vol. 2, ed. by R.W. Carlson (Elsevier-Pergamon, Oxford, 2003), p. 547
4. W.F. McDonough, R. Arevalo, J. Phys. Conf. Ser. **136**(2008). https://doi.org/10.1088/1742-6596/136/2/022006
5. B.A. Baffet, H.E. Huppert, J.R. Lister, A.W. Woods, Nature **356**, 329 (1992)
6. B.L.N. Kennett, Geophys. J. Int. **132**, 374 (1998)
7. G. Masters, D. Gubbins, Phys. Earth Planet. Inter. **140**, 159 (2003)
8. A.M. Dziewonski, D.L. Anderson, Phys. Earth Planet. Inter. **25**, 297 (1981)
9. A. Placci, E. Zavattini, On the possibility of using high-energy neutrinos to study the Earth's interior. CERN Report (1973). https://cds.cern.ch/record/2258764
10. L.V. Volkova, G.T. Zatsepin, Izv. Akad. Nauk, Ser. Fiz. **38N5**, 1060 (1974)
11. I.P. Nedyalkov, Notes on neutrino tomography. Acad. Bulg. Sci. **34**, 177 (1981)
12. I.P. Nedyalkov, preprint JINR (Dubna), JINR-P2-81-645 (1981)
13. I.P. Nedyalkov, On the study of the Earth composition by means of neutrino experiments, in Balatonfuered 1982, Proc. Neutrino '82, vol. 1, p. 300 (1982)
14. I.P. Nedialkov, Measurement of projected mass density—a basic problem of neutrinogeophysics. Acad. Bulg. Sci. **36**, 1515 (1983)
15. A. De Rujula, S.L. Glashow, R.R. Wilson, G. Charpak, Phys. Rep. **99**, 341 (1983)
16. T.L. Wilson, Nature **309**, 38 (1984)
17. G. A. Askar'yan, Usp. Fiz. Nauk **144**, 523 (1984) [Sov. Phys. Usp. **27**, 896 (1984)]
18. A.B. Borisov, B.A. Dolgoshein, A.N. Kalinovsky, Yad. Fiz. **44**, 681 (1986)
19. A.B. Borisov, B.A. Dolgoshein, Phys. At. Nucl. **56**, 755 (1993)
20. W. Winter, Earth Moon Planets **99**, 285 (2006)
21. C. Kuo et al., Earth Planet. Sci. Lett. **133**, 95 (1995)
22. P. Jain, J.P. Ralston, G.M. Frichter, Astropart. Phys. **12**, 193 (1999)
23. M.M. Reynoso, O.A. Sampayo, Astropart. Phys. **21**, 315 (2004)
24. M.C. Gonzalez-Garcia, F. Halzen, M. Maltoni, H.K.M. Tanaka, Phys. Rev. Lett. **100**, 061802 (2008). arXiv:0711.0745 [hep-ph]
25. M. Tanabashi et al. [Particle Data Group], Phys. Rev. D **98**, 030001 (2018). https://doi.org/10.1103/PhysRevD.98.030001. See therein the review "Neutrino Masses, Mixing and Oscillations" by K. Nakamura and S.T. Petcov
26. T.K. Gaisser, M. Honda, Annu. Rev. Nucl. Part. Sci. **52**, 153–199 (2002). arXiv:hep-ph/0203272
27. R. Abbasi et al. [IceCube Collab.], Astropart. Phys. **35**, 615 (2012)
28. M.G. Aartsen et al. [IceCube Collab.], Phys. Rev. Lett. **120**, 071801 (2018)
29. S. Blot [for the IceCube-PINGU Collab.], *talk given at the XXIX Int. Conference on Neutrino Physics and Astrophysics, Chicago, June 22–July 2, 2020 (virtual conference)*. https://doi.org/10.5281/zenodo.3959546
30. M.G. Aartsen et al. [IceCube-PINGU], Letter of Intent: The Precision IceCube Next Generation Upgrade (PINGU). arXiv:1401.2046 [physics.ins-det]
31. M.G. Aartsen et al., [IceCube], J. Phys. G **44**, 054006 (2017). arXiv:1607.02671 [hep-ex]
32. S. Adrian-Martinez et al. [KM3Net], Letter of intent for KM3NeT 2.0. J. Phys. G **43**, 084001 (2016). arXiv:1601.07459 [astro-ph.IM]
33. K. Abe et al. [Hyper-Kamiokande], arXiv:1805.04163 [physics.ins-det]
34. M. Ishitsuka [on behalf of the Hyper-Kamiokande Proto-Collab.], *talk given at the XXIX Int. Conference on Neutrino Physics and Astrophysics, Chicago, June 22–July 2, (2020) (virtual conference)*. https://doi.org/10.5281/zenodo.3959585
35. B. Abi et al. [DUNE], arXiv:1807.10334 [physics.ins-det]
36. A. Donini, S. Palomares-Ruiz, J. Salvado, Nat. Phys. **15**, 37 (2019). https://doi.org/10.1038/s41567-018-0319-1 arXiv:1803.05901 [hep-ph]
37. B. Luzum et al., Celest. Mech. Phys. **110**, 110 (2011)
38. H.USAO, USNO, UKHO, The Astronomical Almanac. http://asa.usno.navy.mil/
39. W. Chen, J. Ray, W.B. Shen, C.L. Huang, J. Geod. **89**, 179 (2015)
40. M.G. Aartsen et al., [IceCube]. Phys. Rev. Lett. **117**, 071801 (2016). arXiv:1605.01990 [hep-ex]

41. W. Winter, Nucl. Phys. B **908**, 250–267 (2016). arXiv:1511.05154 [hep-ph]. [39]
42. S. Bourret et al., [KM3NeT], J. Phys. Conf. Ser. **888**, 012114 (2017). arXiv:1702.03723 [physics.ins-det]
43. A. Kumar, S.K. Agarwalla, JHEP **08**, 139 (2021). arXiv:2104.11740 [hep-]
44. T. Ohlsson, H. Snellman, Phys. Lett. B **474** (2000). arXiv:hep-ph/9912295 153 [erratum: Phys. Lett. B **480** (2000), 419–419]
45. M. Sajjad Athar, M. Honda, T. Kajita, K. Kasahara, S. Midorikawa, Phys. Lett. B **718**, 1375–1380 (2013). arXiv:1210.5154 [hep-ph]
46. P. Yanez, A. Kouchner, Adv. High Energy Phys. **27**, 2015 (1968)
47. J. Brunner [KM3NeT], PoS **ICRC2015**,1140 (2016) . https://doi.org/10.22323/1.236.1140
48. M.C. Gonzalez-Garcia, M. Maltoni, T. Schwetz, JHEP **11**, 052 (2014). arXiv:1409.5439 [hep-ph]
49. S. Ahmed et al., [ICAL], Pramana **88**, 79 (2017). arXiv:1505.07380 [physics.ins-det]
50. S.K. Agarwalla, T. Li, O. Mena, S. Palomares-Ruiz, arXiv:1212.2238 [hep-ph]
51. C. Rott, A. Taketa, D. Bose, Sci. Rep. **5**, 15225 (2015). https://doi.org/10.1038/srep15225 arXiv:1502.04930 [physics.geo-ph]
52. S. Bourret, J. Coelho, E. Kaminski, V. Van Elewyck, PoS **ICRC2019**, 1024 (2020). https://doi.org/10.22323/1.358.1024
53. S. Choubey, P. Ghoshal, S.T. Petcov, studies performed in the period 2008–2011, unpublished
54. S. Choubey, S.T. Petcov, studies performed in 2014, unpublished
55. M. Honda, M. Sajjad Athar, T. Kajita, K. Kasahara, S. Midorikawa, Phys. Rev. D **92** 023004 (2015). arXiv:1502.03916 [astro-ph.HE]. The tables for the fluxes and production height calculated for the Frejus/Gran Sasso cite are available in the web page, http://www.icrr.u-tokyo.ac.jp/~mhonda cited in this paper
56. F. Capozzi, E. Lisi, A. Marrone, J. Phys. G **45**, 024003 (2018). arXiv:1708.03022 [hep-ph]
57. T. Ohlsson, W. Winter, Phys. Lett. B **512**, 357 (2001). arXiv:hep-ph/0105293
58. S.T. Petcov, Phys. Lett. B **434**, 321 (1998). https://doi.org/10.1016/S0370-2693(98)00742-4. arXiv:hep-ph/9805262; Phys. Lett. B **444** (1998) 584 (Erratum)
59. M.V. Chizhov, S.T. Petcov, Phys. Rev. Lett. **83**, 1096 (1999). arXiv:hep-ph/9903399
60. M.V. Chizhov, S.T. Petcov, Phys. Rev. D **63**, 073003 (2001). arXiv:hep-ph/9903424
61. M. Chizhov, M. Maris, S.T. Petcov, arXiv:hep-ph/9810501
62. E.K. Akhmedov, M. Maltoni, A.Y. Smirnov, JHEP **05**, 077 (2007). arXiv:hep-ph/0612285
63. E.K. Akhmedov, M. Maltoni, A.Y. Smirnov, Phys. Rev. Lett. **95**, 211801 (2005). arXiv:hep-ph/0506064
64. L. Wolfenstein, Phys. Rev. D **17**, 2369 (1978)
65. L. Wolfenstein, in ed. by E.C. Fowler*Proceedings of the 8th International Conference on Neutrino Physics and Astrophysics—"Neutrino'78"* (Purdue University Press, West Lafayette, 1978), p. C3
66. V. Barger et al., Phys. Rev. D **22**, 2718 (1980)
67. P. Langacker, J.P. Leveille, J. Sheiman, Phys. Rev. D **27**, 1228 (1983)
68. J. Badro et al., Proc. Natl. Acad. Sci. USA **112**(40), 12310–12314 (2015)
69. E. Kaminski, M. Javoy, Earth Planet. Sci. Lett. **365**, 97–107 (2013)
70. T. Sakamaki et al., Earth Planet. Sci. Lett. **287**, 293–297 (2009)
71. https://earthref.org/GERMRD/datamodel/ (cit. on pp. 114, 115)
72. S.P. Mikheev, A.Y. Smirnov, Sov. J. Nucl. Phys. **42**, 913 (1985)
73. G.L. Fogli, E. Lisi, A. Marrone, D. Montanino, A. Palazzo, A.M. Rotunno, Phys. Rev. D **86**, 013012 (2012). arXiv:1205.5254 [hep-ph]
74. E. Lisi, D. Montanino, Phys. Rev. D **56**, 1792 (1997). arXiv:hep-ph/9702343
75. F. Capozzi, E. Lisi, A. Marrone, Phys. Rev. D **91**, 073011 (2015). arXiv:1503.01999 [hep-ph]
76. F. Capozzi, E. Di Valentino, E. Lisi, A. Marrone, A. Melchiorri, A. Palazzo, Phys. Rev. D **95**, 096014 (2017). arXiv:1703.04471 [hep-ph]. Phys. Rev. D 101 (2020) 116013 (addendum). arXiv:2003.08511 [hep-ph]
77. F. Capozzi, E. Di Valentino, E. Lisi, A. Marrone, A. Melchiorri, A. Palazzo, arXiv:2107.00532 [hep-ph]
78. E.K. Akhmedov, A. Dighe, P. Lipari, A.Y. Smirnov, Nucl. Phys. B **542**, 3 (1999). arXiv:hep-ph/9808270
79. J. Bernabeu, S. Palomares Ruiz, S.T. Petcov, Nucl. Phys. B **669**, 255 (2003). arXiv:hep-ph/0305152
80. S.T. Petcov, T. Schwetz, Nucl. Phys. B **740**, 1 (2006). arXiv:hep-ph/0511277
81. G.L. Fogli, E. Lisi, A. Marrone, D. Montanino, A. Palazzo, Phys. Rev. D **66**, 053010 (2002)
82. I. Esteban, M.C. Gonzalez-Garcia, M. Maltoni, T. Schwetz, A. Zhou, JHEP **09**, 178 (2020). arXiv:2007.14792 [hep-ph]
83. J. Hofestädt, M. Bruchner, T. Eberl, PoS **ICRC2019**, 911 (2020). arXiv:1907.12983 [hep-ex]
84. K.J. Kelly, P.A.N. Machado, I. Martinez-Soler, Y.F. Perez-Gonzalez, arXiv:2110.00003 [hep-ph]
85. P.B. Denton, R. Pestes, arXiv:2110.01148 [hep-ph]
86. R. Gandhi, P. Ghoshal, S. Goswami, P. Mehta, S.U. Sankar, S. Shalgar, Phys. Rev. D **76**(2007). https://doi.org/10.1103/PhysRevD.76.073012 arXiv:0707.1723 [hep-ph]
87. R. Gandhi, P. Ghoshal, S. Goswami, S.U. Sankar, Phys. Rev. D **78**(2008). https://doi.org/10.1103/PhysRevD.78.073001 arXiv:0807.2759 [hep-ph]
88. M. Honda, T. Kajita, K. Kasahara, S. Midorikawa, In a 3-dimensional scheme. Phys. Rev. D **70**, 043008 (2004). arXiv:astro-ph/0404457
89. A. Rubbia, arXiv:hep-ph/0402110
90. A. Bueno et al., JHEP **0704**, 041 (2007). arXiv:hep-ph/0701101
91. D.B. Cline, F. Raffaelli, F. Sergiampietri, JINST **1**, T09001 (2006). arXiv:astro-ph/0604548
92. A. Ereditato, A. Rubbia, Nucl. Phys. Proc. Suppl. **155**, 233 (2006). arXiv:hep-ph/0510131